# Where and When Does Streamflow Regulation Significantly Affect Climate Change Outcomes in the Columbia River Basin?

Jane Harrell[1,1], Bart Nijssen[1,1], and Chris Frans[2,2]

[1]University of Washington
[2]United States Army Corps of Engineers

November 30, 2022

**Abstract**

The Columbia River basin is a large transboundary basin located in the Pacific Northwest. The basin spans seven US states and one Canadian province, encompassing a diverse range of hydroclimates. Strong seasonality and complex topography are projected to give rise to spatially heterogeneous climate effects on unregulated streamflow. The basin's water resources are economically critical, and regulation across the domain is extensive. Many sensitivity studies have investigated climate impacts on the basin's naturalized hydrology; however, few have considered the large role of regulation. This study investigates where and when regulation affects projected changes in streamflow by comparing climate outcomes across 80-member ensembles of unregulated and regulated streamflow projections at 75 sites across the basin. Unregulated streamflow projections are taken from an existing dataset of climate projections derived from Coupled Model Intercomparison Project version 5 Global Climate Models. Regulated streamflow projections were modeled by the US Army Corps of Engineers and the US Bureau of Reclamation by using these unregulated flows as input to hydro-regulation models that simulate operations based on current and historical water demands. Regulation dampens shifts in winter and summer streamflow volumes. Regulation generally attenuates changes in cool-season high flow extremes but amplifies shifts in warm-season and annual high flow extremes at historically snow-dominant headwater reservoirs. Regulation reduces dry-season low flow changes in headwater tributaries where regulation is large but elsewhere has little effect on changes in low flows. Results highlight the importance of accounting for water management in climate sensitivity analysis particularly in snow-dominant basins.

## Hosted file

essoar.10510745.2.docx available at https://authorea.com/users/549096/articles/607683-where-and-when-does-streamflow-regulation-significantly-affect-climate-change-outcomes-in-the-columbia-river-basin

Posted on 30 Nov 2022 — CC-BY 4.0 — https://doi.org/10.1002/essoar.10510745/v2 — This a preprint and has not been peer reviewed. Data may be preliminary.

Jane Harrell[1], Bart Nijssen[1], Chris Frans[2]

[1]Department of Civil and Environmental Engineering, University of Washington, Seattle, WA, USA

[2]Seattle District, U.S. Army Corps of Engineers, Seattle, WA, USA

Corresponding author: Jane Harrell (harrellj@uw.edu)

Key Points:

- Regulation dampens future winter and summer volume changes where the degree of upstream regulation is large.
- Regulation dampens cool-season high flow extreme increases and amplifies warm-season increases at snow-dominant headwater basins.
- Regulation dampens low flow changes in tributaries with a large degree of upstream regulation but has little to no effect elsewhere.

**Abstract**

The Columbia River basin is a large transboundary basin located in the Pacific Northwest. The basin spans seven US states and one Canadian province, encompassing a diverse range of hydroclimates. Strong seasonality and complex topography are projected to give rise to spatially heterogeneous climate effects on unregulated streamflow. The basin's water resources are economically critical, and regulation across the domain is extensive. Many sensitivity studies have investigated climate impacts on the basin's naturalized hydrology; however, few have considered the large role of regulation. This study investigates where and when regulation affects projected changes in streamflow by comparing climate outcomes across 80-member ensembles of unregulated and regulated streamflow projections at 75 sites across the basin. Unregulated streamflow projections are taken from an existing dataset of climate projections derived from Coupled Model Intercomparison Project version 5 Global Climate Models. Regulated streamflow projections were modeled by the US Army Corps of Engineers and the US Bureau of Reclamation by using these unregulated flows as input to hydro-regulation models that simulate operations based on current and historical water demands. Regulation dampens shifts in winter and summer streamflow volumes. Regulation generally attenuates changes in cool-season high flow extremes but amplifies shifts in warm-season and annual high flow extremes at historically snow-dominant headwater reservoirs. Regulation reduces dry-season low flow changes in headwater tributaries where regulation is large but elsewhere has little effect on changes in low flows. Results highlight the importance of accounting for water management in climate sensitivity analysis particularly in snow-dominant basins.

## 1 Introduction

The Columbia River basin is responsible for 77% of coastal drainage in the Northwestern US (Barnes et al., 1972) and is the sixth largest basin by drainage area in the United States (Kammerer, 1990). Located in the Pacific Northwest, the basin spans seven states and straddles the US-Canadian border, encompassing a diverse range of hydroclimates and topography. The 4th National Climate Assessment states that 21st century temperatures are projected to rise for all greenhouse gas emission scenarios and extreme precipitation events are increasing (Reidmiller et al., 2018). The natural hydrology of the Pacific Northwest is particularly sensitive to shifts in climate due to the region's complex topography, the prominent role of snow in warm-season streamflow, and strong seasonality of the annual hydrograph (Elsner et al., 2010; Vano, 2015).

Over the past century, the Pacific Northwest has warmed by nearly 1ºC, and temperatures are projected to continue to rise (May et al., 2018). At upper elevations, warming has already resulted in declines in glacial extent (Frans et al., 2018; Moore et al., 2020) and snowpack (Mote et al., 2018) and is projected to cause significant depletions in seasonal snowpack (Elsner et al., 2010; Gergel et al., 2017; Lute et al., 2015; RMJOC, 2018). At lower elevations, more cool-season precipitation will likely fall as rain rather than snow (Musselman et al., 2018; Salathé et al., 2018). Mountain snowpack serves as a natural reservoir of fresh water and diminishing snowpack could lead to more frequent and severe drought events (Chegwidden et al., 2019; Leppi et al., 2012; RMJOC, 2018; Tohver et al., 2014). Seasonal precipitation patterns are projected to amplify under climate change. Precipitation is projected to increase in the autumn, winter, and spring, and decrease in the summer during the dry season (RMJOC, 2018; Rupp et al., 2016; Tohver et al., 2014). The largest seasonal increases are likely to occur in winter, which historically is the season with the largest total precipitation. Changes in annual precipitation patterns and depletions in snowpack will shift peak streamflow timing earlier in the water year for snow dominant and transient rain-snow watersheds (Chegwidden et al., 2019; Fritze et al., 2011; Hamlet et al., 2010; Payne et al., 2004; Stewart et al., 2005). Peak timing shifts will likely be more pronounced in transient watersheds where winter temperatures are at or near freezing and therefore more sensitive to warming (Bureau of Reclamation, 2016; Vano et al., 2015). Extreme precipitation events are increasing (IPCC, 2014; May et al., 2018; Warner et al., 2017), and are projected to lead to substantially more severe flood events (Salathé et al., 2014). Queen et al. (2021) projected pervasive increases in Columbia River basin flood magnitudes based on unregulated streamflow projections.

Throughout the past century, expansive water resource infrastructure has changed the streamflow regime by creating man-made reservoirs and altering flows. While climate is a primary driver of natural basin hydrology, extensive regulation modulates this natural hydrology and thus streamflow (Figure 1; Arheimer et al., 2017). The Columbia River basin is heavily regulated by federal and state agencies and private utilities for a range of system objectives including flood risk management, hydropower, irrigation, navigation, fish passage, and recreation. More than 250 reservoirs exist across the system and streamflow regulation sustains an economically critical food-water-energy nexus. Columbia River system operations follow transnational guidelines defined by the Columbia River Treaty, an international agreement between the US and Canada on how water is allocated across the US-Canadian border. Ratified in 1964, the treaty informs the joint management of three upper Columbia Canadian storage dams to coordinate transboundary flood control and is currently being renegotiated for modernization post-2024 (Stern, 2020).

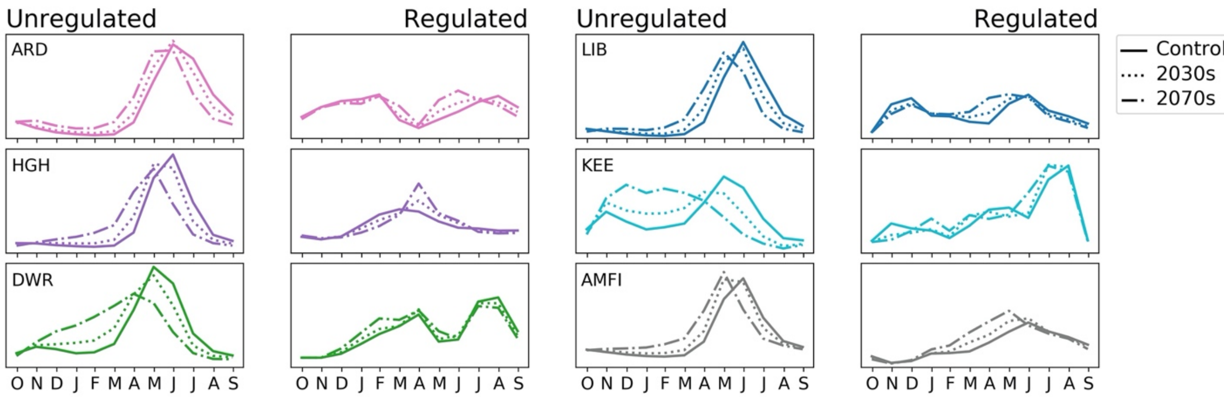


Fig. Annual hydrographs of monthly average streamflow for Arrow Lakes (ARD), Libby (LIB), Hungry Horse (HGH), Keechelus (KEE), Dworshak (DWR), and American Falls (AMFI) and the three periods examined: the control period (1976-2005), 2030s (2020-2049), and 2070s (2060-2089). Monthly averages are taken from the median of each ensemble. For each location, the left panel shows the unregulated hydrograph, and the right panel shows the regulated hydrograph.

Climate change impacts on Columbia River basin naturalized or unregulated streamflow have been extensively studied; however, only a limited number of large-scale studies have considered the large role of regulation. To test the reliability and vulnerability of Columbia River system operations under changing historical conditions, Jones and Hammond (2020) investigated observed intra-annual timing of reservoir inflows and outflows. Between 1950 and 2012, May through October inflows declined but outflows increased due to low flow augmentation. Zhou et al. (2018) investigated the effect of regulation on the timing of hydrologic regime shifts for large basins across the western US. Their study used climate projections from three Coupled Model Intercomparison Project version 5 (CMIP5) global climate models (GCMs) for Representative Concentration Pathway (RCP) 4.5 and 8.5 emissions scenarios. GCM meteorology was statistically downscaled to the 1/8-degree grid resolution. Regulated flows were simulated by the Model for Scale Adaptive River Transport (Li et al., 2013) Water Management (Voisin et al., 2013a) model (MOSART-WM); a simplified hydro-regulation model that uses operational rules based on historical monthly mean inflows and water demands. Zhou et al. (2018) found that for the Columbia River basin, regulation delayed the timing of regime shifts for all seasons except autumn. Studies in subbasins west of the Cascade Mountain range have also shown large differences between projected changes in unregulated and regulated streamflow extremes where, in some cases, regulation amplifies the climate signal (Lee et al., 2016, 2018). Singh and Basu (2022) analyzed historical seasonal streamflow trends in neighboring natural and regulated watersheds across North America. They showed that regulation effects on seasonal streamflow trends vary widely across space and time ranging from amplification to no effect to dampening.

As climate change poses potential challenges for managed freshwater systems, concerns regarding where and when climate impacts will manifest and what they mean for the future of water resources are ever-growing. Large-scale climate sensitivity studies that do not account for regulation effects on streamflow may lead to inaccurate characterizations of projected outcomes. To investigate where and when extensive regulation modifies climate impacts on Columbia River basin streamflow, this study uses two 80-member ensembles of unregulated and regulated streamflow projections developed from 10 CMIP5 GCM projections for the RCP 8.5 emissions scenario (RMJOC, 2018; RMJOC, 2020) to compare climate outcomes under unregulated and regulated conditions. Regulated flow projections were modeled by the US Army Corps of Engineers (USACE) and the US Bureau of Reclamation (USBR) using hydro-regulation models that are used by USACE and USBR to support long- and short-term federal water management planning. These models use operational rule-curves based on current and historical water management objectives that vary temporally and spatially and account for local and system-wide flood risk management, hydropower, irrigation, navigation, and ecological constraints (RMJOC, 2020). Operational rule-curves are based on current and historical water demands and do not change to account for future changing conditions.

This study seeks to answer two key questions: 1) How does regulation modify projections of streamflow volumes and extreme streamflow events under climate change? 2) How do the signatures of climate change and hydro-regulation vary seasonally and across the domain? We address these questions by comparing projected climate impacts on seasonal volumes and high and low flow extremes for unregulated conditions and regulated conditions. We investigate changes in extremes for 51 diverse sites across the basin where hydro-regulation was modeled at a daily time step. Seasonal volume changes are examined for 75 sites using output from hydro-regulation models at both a daily and monthly time step. Outcomes for the 2030s (2020-2049) and the 2070s (2060-2089) are compared to the control period (1976-2005), and we test relationships to river network location and the level of regulation by grouping locations by region and the degree of upstream regulation, respectively. The control period is selected to represent the most recent 30-year period in the historical streamflow used to validate simulated flows (RMJOC, 2018). The 2030s and 2070s are selected to represent the near future and far future, respectively. Analysis is performed for water years rather than calendar years. A water year is a 12-month period used by hydrologists to represent temporal precipitation patterns that influence the water cycle (e.g., wet-season winter snow accumulation and dry-season summer snow melt) and is defined as October 1 of the previous calendar year through

September 30 of the given year.

# 2 Methods

## 2.1 Study Area

The Columbia River basin is a transnational river system covering 673 thousand km$^2$ of the Pacific Northwest. The basin encompasses a diverse range of hydroclimates from arid lowlands to glaciated mountain regions. The Cascade and Rocky Mountain ranges pass through the western and eastern edges of the basin, respectively, and high elevation snowpack supplies much of the basin's freshwater through the spring freshet. Three hydrologic regimes exist across the domain (Hamlet and Lettenmaier, 2007): the rain-dominant regime where streamflow peaks in the cool-season primarily driven by rainfall; the transient regime where two annual peak streamflow pulses result from cool-season rainfall and warm-season snowmelt; and the snow-dominant regime where streamflow peaks in the warm-season primarily driven by snowmelt (Elsner et al., 2010). These three regimes can be distinguished by the ratio of peak snow water equivalent (SWE) to cool-season precipitation (Barnet et al, 2005). Pacific Northwest peak SWE typically occurs around April 1. Following the work of Mantua et al. (2010), we classify hydrologic regimes for each 30-year period by the ensemble median ratio of drainage area-averaged April 1 SWE to drainage-area averaged October through March precipitation (SWE/P) where SWE/P less than 0.1 indicates a rain-dominant regime; SWE/P between 0.1 and 0.4 indicates a transient regime; and SWE/P greater than 0.4 indicates a snow-dominant regime (Figure 2).

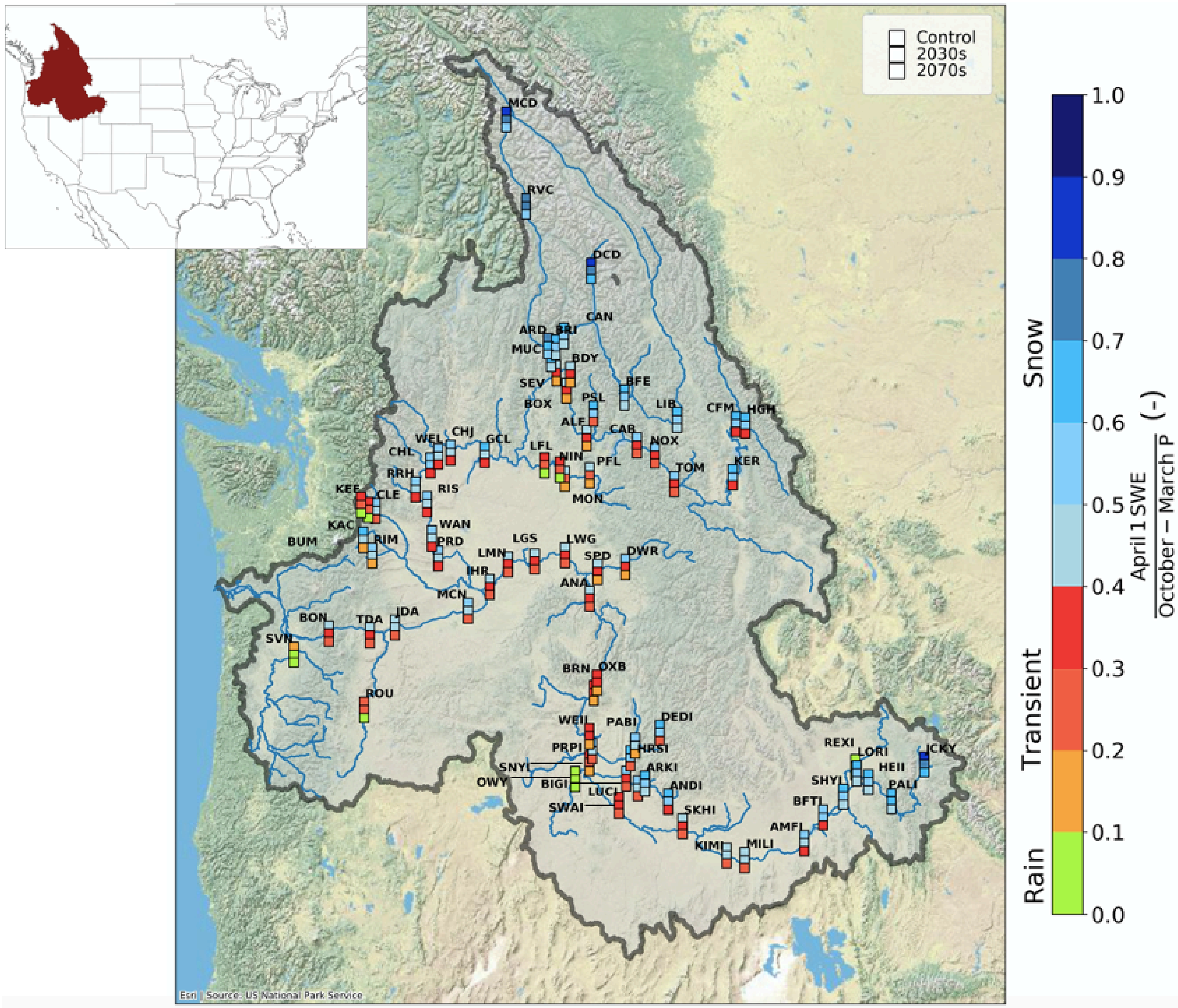


Fig. Map of the Columbia River basin and hydrologic regime ratios for the 75 sites and three periods investigated in this study. The basin is located in the Pacific Northwest region of the US straddling the US-Canadian border. Regime classification color scheme adapted from Mantua et al. (2010). Base map provided by Esri (2009). For location details including drainage area see Table S1 of Supporting Information.

2.2 Location and Groupings

*2.2.1 Regions*

The hydroclimate across the domain is diverse, and system operations vary widely depending on the authorized purposes of water management infrastructure and regional water demands. To test the relationship between regulation effects and river network location, sites are grouped into ten regions defined by location on a tributary or the mainstem (Figure 3a).

*2.2.2 Degree of Upstream Regulation*

Regulation effects on streamflow can be attributed to temporal reservoir storage and delayed releases that alter streamflow timing (Grill et al., 2019). The degree of upstream regulation (DOR) is a measure of annual storage effects on unregulated streamflow and is defined as total upstream storage capacity normalized by annual streamflow volume (Dynesius and Nillson, 1994; Grill et al., 2019; Lehner et al., 2011). Higher DOR indicates greater capacity to store water throughout the water year and as a result, larger regulation effects on the streamflow regime. We group locations by their DOR to test the relationship between annual storage effects and regulated climate outcomes (Figure 3b), with DOR calculated as

$\mathrm{DO}R_j = \frac{\sum_{i=1}^{n} SV_i}{AV_j}$, #(1)

where $\mathrm{DO}R_j$ is the DOR at site $j$, $SV_i$ is the storage volume of any reservoir upstream of site $j$, $n$ is the total number of reservoirs upstream of site $j$ and $AV_j$ is the unregulated annual streamflow volume at site $j$ (Lehner et al., 2019). To group sites with similar DOR, we applied equation (1) during the control period and binned the range of DOR across all sites into 4 groupings of equal intervals: 0-30%; 30-60%; 60-90%; and 90-120%.

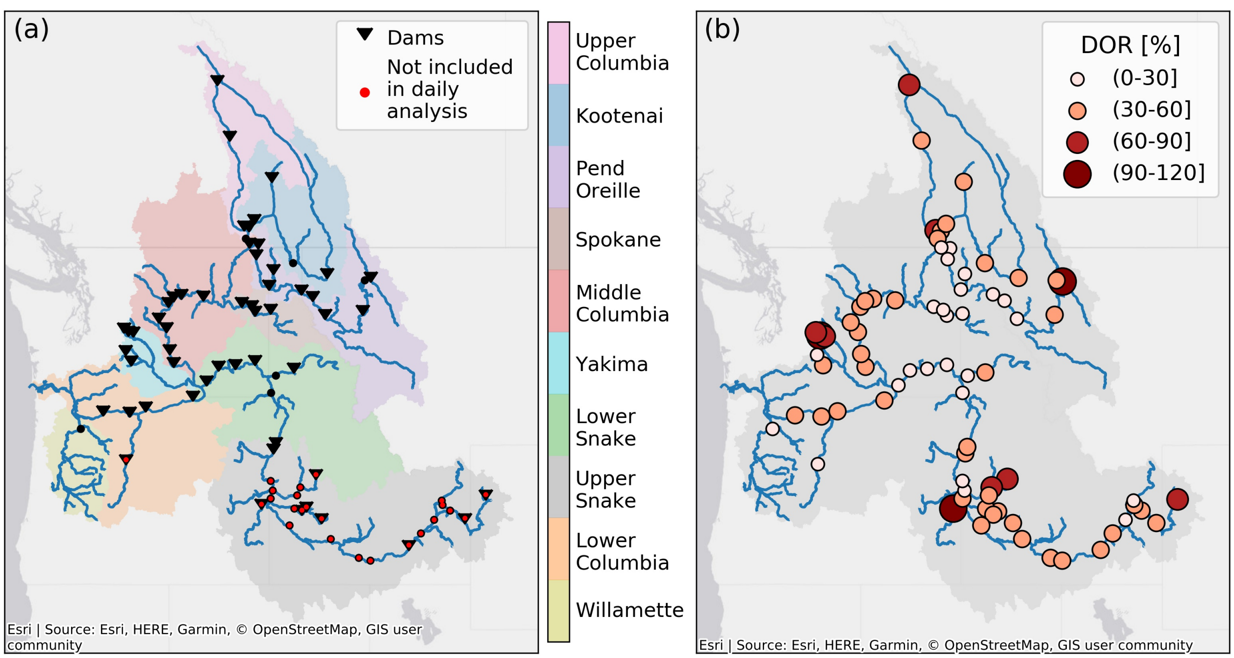


Fi

. Maps of the spatial groupings used in this study: (a) analysis regions; (b) degree of upstream regulation (DOR). Base map provided by Esri (2011).

2.3 Seasonal Volumes

Reservoir releases vary widely throughout the year and operational constraints are highly seasonally dependent. As a result, changes in seasonal streamflow volumes have been identified by stakeholders as indicators of system vulnerability for a wide range of water management objectives (RMJOC, 2020). The hydro-regulation models used to generate the regulated flow ensemble examined in this study use rule-curves and other operational targets that vary by season based on historical hydroclimate (RMJOC, 2020); however, the seasonality of unregulated hydrographs is projected to shift under climate change (Figure 1) and large shifts in seasonal volumes may drive large regulation effects. We compare climate change effects on seasonal volumes by examining the relative seasonal volume change, defined as the ratio of future seasonal volumes to control period volumes, under both unregulated conditions and regulated conditions for September, October, November (SON; autumn); December, January, February (DJF; winter); March, April, May (MAM; spring); and June, July, August (JJA; summer).

2.4 Level of Seasonal Volume Regulation

The level of seasonal volume regulation (LRsv) is defined as the ratio of regulated seasonal volume to unregulated seasonal volume,

$$LR_{\mathrm{sv}} = \frac{\text{Regulated Seasonal Volume}}{\text{Unregulated Seasonal Volume}}, \#(2)$$

where the seasonal volume is the total amount of flow observed at one of the 75 sites identified in Figure 2. LRsv values greater than 1 indicate the regulated seasonal volume exceeds the unregulated seasonal volume while LRsv values less than 1 indicate the regulated seasonal volume is less than the unregulated seasonal volume. We compare control period LRsv to future LRsv to examine how the relationship between regulated and unregulated volumes is changing in the future. It is important to keep in mind that both the numerator and denominator change when applying equation (2) to different periods.

2.5 Extremes

An analysis of changes in extremes can provide critical information for adaptation planning given extensive flood risk management practices and competing demands for water. We investigate regulation effects on high flow extremes by comparing relative changes in annual peak flows with a 50-year return period (Q50RP) under regulated conditions to those under unregulated conditions. The Log-Pearson 3 (LP3) distribution curve is fit to regulated and unregulated annual maximum flow time series for each 30-year period (Text S1 of Supporting Information). By using a 30-year sample size rather than a larger (e.g., 50 or 75-year) sample size, we limit the effects of non-stationarity in sample statistics used to generate the LP3 curve. We examine 50-year return period (2% annual exceedance probability) maxima rather than 100-year return period maxima due to lower confidence in the 1% annual exceedance probability that results from using a 30-year sample size. From the LP3 distributions, 50-year return period peak flow changes are investigated by calculating the ratio of future to control period Q50RP. The LP3 fit for unregulated high flow extremes is recommended by United States Geological Survey (USGS) Bulletin 17C (England et al., 2018) which established federal guidelines for flood frequency analysis. Regulated high flow frequency curves are typically generated using graphical fitting methods; however, we use the LP3 distribution to fit both unregulated and regulated high flow frequency curves in order to apply a consistent method across a large number of sites. Warming temperatures will shift streamflow maxima towards winter where they historically occurred in spring (indicated by widespread regime shifts across the domain as shown in Figure 2), and seasonally varying operations could explain large changes in regulated Q50RP. To identify seasonal climatic changes and operations that drive annual Q50RP changes, we also examine changes in cool-season (October-March) Q50RP and warm-season (April-September) Q50RP.

We investigate regulation effects on low flow extremes similarly, by comparing relative changes in 7-day minimum flows with a 10-year return period (7Q10) under regulated conditions to those under unregulated conditions. The LP3 distribution curve is fit to regulated and unregulated 7-day minimum flow time series for each 30-year period (Text S2 of Supporting Information). From the LP3 distributions, we examine changes in the 10-year return period 7-day minimum by calculating the ratio of future to control period 7Q10. High snow dominance can lead to annual minimums occurring during cool-season snowpack accumulation (Tohver et al. 2014; see Figure 1). Shifts in dry-season low flow extremes can indicate ecosystem vulnerability and motivate changes in late summer and early autumn ecological operations. Rather than taking the 7Q10 from the annual time series, we limit our analysis to the dry-season (July-October) when low flow operational constraints occur across the domain (RMJOC, 2020). The Kolmogorov-Smirnov (KS) and probability plot correlation coefficient (PPCC) goodness of fit tests (Stedinger et al., 1993) are performed to test the suitability of the LP3 analytical curves for fitting the unregulated and regulated low and high flow extreme time series (Figures S3-S14 of Supporting Information).

## 2.6 Level of Q50RP Regulation

Similar to the level of seasonal volume regulation defined in section 2.4, we define the level of Q50RP regulation ($\mathrm{LR}_{\mathrm{Q50RP}}$) as the ratio of regulated Q50RP to unregulated Q50RP,

$$LR_{Q50RP} = \frac{Regulated\ Q50RP}{Unregulated\ Q50RP}.\#(3)$$

$\mathrm{LR}_{\mathrm{Q50RP}}$ greater than 1 indicates that the regulated Q50RP exceeds the unregulated Q50RP while $\mathrm{LR}_{\mathrm{Q50RP}}$ less than 1 indicates the regulated Q50RP is less than the unregulated Q50RP. Because the Q50RP amounts are determined independently from the regulated and unregulated flow time series, they do not necessarily denote the same event.

# 3 Data

## 3.1 Unregulated Streamflow Projections

Unregulated streamflow projections are taken from Chegwidden et al. (2017). This dataset consists of Columbia River basin simulated streamflow at a daily time step from the Precipitation Runoff Modeling System (PRMS; Leavesly et al., 1983) and Variable Infiltration Capacity model (VIC; Liang et al., 1994). Both PRMS and VIC were forced using statistically downscaled CMIP5 GCM projections for the RCP 4.5 and RCP 8.5 emissions scenario. For the purposes of this study, we limit our analysis to emissions scenario RCP 8.5 which represents the amount of radiative forcing that is projected to occur if no effort is made to decrease greenhouse gas emissions. GCM forcings were statistically downscaled and bias-corrected at the $1/16^{\text{th}}$ degree grid resolution using two different methods: the multivariate adaptive constructed analogs (MACA) method, and the bias correction, spatial disaggregation (BCSD; Wood et al., 2004) downscaling method. Ten GCMs, two meteorological downscaling methods, two hydrology models, and three model parameter sets for the VIC model resulted in an 80-member ensemble of unregulated streamflow projections for RCP 8.5 at locations across the Pacific Northwest (Chegwidden et al., 2019). From this dataset, we analyze streamflow changes at 75 Columbia River basin locations that map to sites where hydro-regulation was modeled by USACE and USBR.

## 3.2 Regulated Streamflow Projections

Regulated streamflow projections were developed by USACE and USBR. With the exception of the Yakima, Upper Snake, and Deschutes, regulation across the basin was simulated at a daily-step using the USACE Hydrologic Engineer Center's Reservoir System Simulations model (HEC-ResSim) (USACE, 2013) developed by USACE for Columbia River basin planning studies (RMJOC, 2020). This model was recently updated with operating rules based on a preferred alternative from a National Environmental Policy Act (NEPA) Environmental Impacts Study of system operations. These include an updated set of operational contstraints and targets for 14 major storage projects that integrate water management for improved anadromous fish habitat and survival (USACE, 2020).

Regulation in the Yakima River basin was simulated by USBR at a daily time step using the RiverWare model (Zagona et al., 2010). The Yakima regulation model was developed to simulate operations and irrigation under 2010 conditions (Bureau of Reclamation, 2010b; RMJOC, 2020). Regulation in the Upper Snake and Deschutes was modeled at a monthly time step using MODSIM (Labadie, 2006) to simulate operations and irrigation under 2008 conditions (Bureau of Reclamation, 2009, 2010a; RMJOC, 2020).

Reservoir storage targets and outflows vary inter-annually, year-to-year, and spatially, specific to in-season forecasts of seasonal runoff. Monthly storage requirements are determined by seasonal runoff volume forecasts (water supply forecasts) that are issued at the beginning of each month. These forecasts are required by the hydro-regulation models as input for flood risk management operations. In-season water supply forecasts for 9 primary storage projects were developed for each projection using principal component regression and the projected hydrologic states. These forecasts were then used as input to the hydro-regulation models to set local and system operational storage requirements across the domain (RMJOC, 2020). While reservoir operational patterns can vary annually and seasonally based on forecasted basin hydrology, the underlying logic for forecast-based storage requirements is defined based on current hydrologic patterns and operational constraints and was not modified to account for shifts in hydrology under climate change. For example, the April-August runoff period, for which forecasts are currently made, may be less relevant in the future when runoff occurs earlier.

The unregulated streamflow projections described in section 3.1 were input into the hydro-regulation models after adjustments were made to account for the effects of irrigation and reservoir evaporation. Irrigation and evaporation extractions were based on historical patterns and depletions adjusted to the level of irrigation of the year 2010 (Bonneville Power Administration, 2011), and were not modified to reflect changes in diversion patterns under climate change. In the Upper Snake, Deschutes, and Yakima subbasins, irrigation withdrawals varied based on historically-observed demand patterns for the projected water year type (i.e., irrigation demand patterns during drought years were different than those during extremely wet years) (Bureau of Reclamation, 2011; RMJOC, 2020). Outside of these subbasins, where irrigation depletions represent a much smaller amount of the annual flow volume, irrigation withdrawals were fixed based on historical depletion levels (RMJOC, 2020). The resulting model output is an 80-member ensemble of regulated Columbia River basin streamflow projections for the RCP 8.5 emissions scenario.

# 4 Results

## 4.1 Seasonal Volumes

### *4.1.1 Regulation Dampens Seasonal Volume Changes in Winter (DJF) and Summer (JJA)*

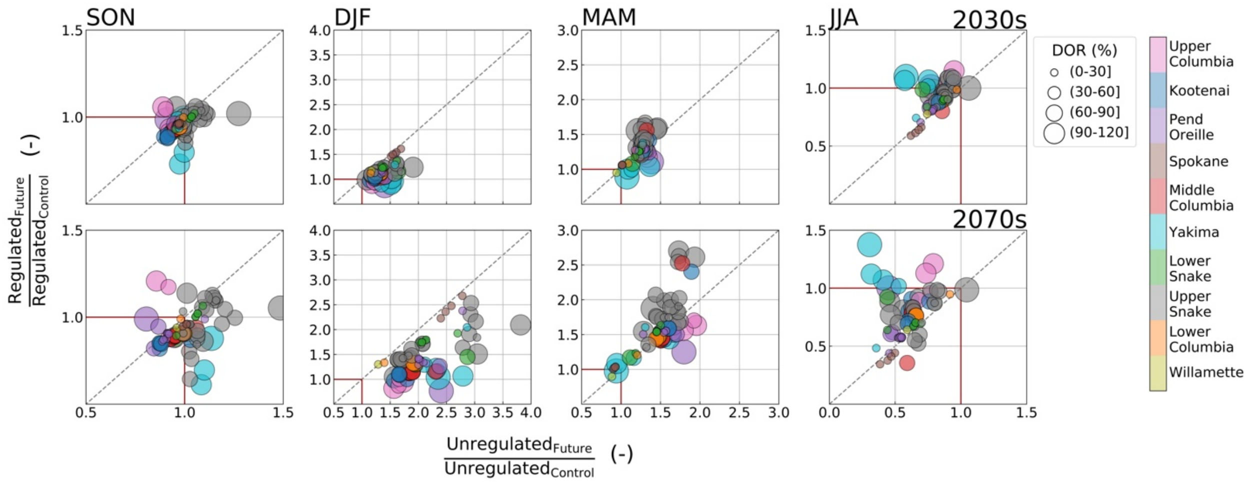


Fig

4. September-November (SON), December-February (DJF), March-May (MAM), and July-August (JJA) seasonal volume ratios for the 2030s (top) and 2070s (bottom) under unregulated conditions (x-axis) and regulated conditions (y-axis). Figure shows the median ratio across the 80-member ensemble. Points are colored by region and sized by the degree of upstream regulation (DOR). In the absence of regulation, points would fall on the dashed 1:1 line. The red box helps to identify the direction of change over time. Points within the red box indicate decreases in future volumes. Points outside of the box indicate increases in future volumes.

We investigate projected seasonal volume changes by taking the ratio of future volumes to control period volumes and compare ratios under unregulated and regulated conditions (Figure 4). Results show changes across all seasons for both conditions by the 2030s and 2070s with the largest shifts occurring by the 2070s. We limit discussion of seasonal volume results to the 2070s, when the greatest changes and differences between unregulated and regulated outcomes occur.

Autumn (SON) unregulated volumes experience the least change out of all seasons (generally less than 25% change across locations) and the direction of change varies spatially. The greatest unregulated volume changes occur in winter (DJF) due to increases in precipitation and more cool-season precipitation falling as rain rather than snow. The unregulated winter signal is strongest in headwater tributaries of the Pend Oreille, Yakima, Spokane, Upper Snake, and Lower Snake subbasins where the hydrologic regime shifts from snow-dominant to transient or transient to rain-dominant. Spring (MAM) unregulated volumes also increase significantly. Snow-dominant sites of the Upper Columbia, Kootenai, and Upper Snake see the largest increases in spring volumes (greater than 90% change) as warming temperatures shift snowmelt timing toward earlier in the water year. In the summer (JJA), unregulated volumes are projected to decrease across locations. The summer months are historically water limited.

Shifts in snowmelt timing coupled with warmer and drier summers drive large reductions in snowmelt-driven streamflow. The greatest summer volume reductions occur at locations in the Yakima, Spokane, Lower Snake, and Pend Oreille where snow-dominant regimes shift to transient by the 2070s (greater than 50% percent change).

The effects of regulation vary spatially in autumn and spring. Autumn unregulated volumes at upstream sites of the Upper Columbia (Mica; MCD and Revelstoke; RVC) decrease by 8-14% but augmentation effects under regulation result in increases of 17-20%. These strong regulation effects diminish downstream (Table S2 of Supporting Information). The opposite effects occur in the Yakima and Upper Snake. Except for a single location in the Yakima, autumn unregulated volumes increase by 2-13% while regulated volumes decrease by 4-38%. In the spring, sites in the Upper Snake that transition from snow-dominant to transient exhibit the greatest differences between unregulated and regulated volume changes where regulation amplifies change (greater relative change under regulation).

Regulation generally dampens change (less relative change under regulation) in winter and summer. Winter unregulated volumes are projected to increase by over 200% at some locations; however, regulation significantly reduces these changes where upstream regulation (DOR) is greater than 30%. Many locations show large winter unregulated volume increases but no projected change or decreases under regulation. These effects predominantly occur downstream of headwater reservoirs in the Upper Columbia, Kootenai, and Pend Oreille that are snow-dominant well into the future or remain snow-dominant through the 2030s and have large DOR. For example, at Hungry Horse (HGH) in the Pend Oreille subbasin, winter unregulated volumes increase by 140%, but regulation results in a 23% decrease. As in winter, summer regulation results in dampening of the climate signal downstream of headwater reservoirs where DOR is large. For some locations in the Yakima and Upper Columbia, summer low flow augmentation results in future summer volume increases where unregulated volumes decrease.

*4.1.2 Level of Seasonal Volume Regulation Explains Large Regulation Effects in Winter (DJF) and Summer (JJA)*

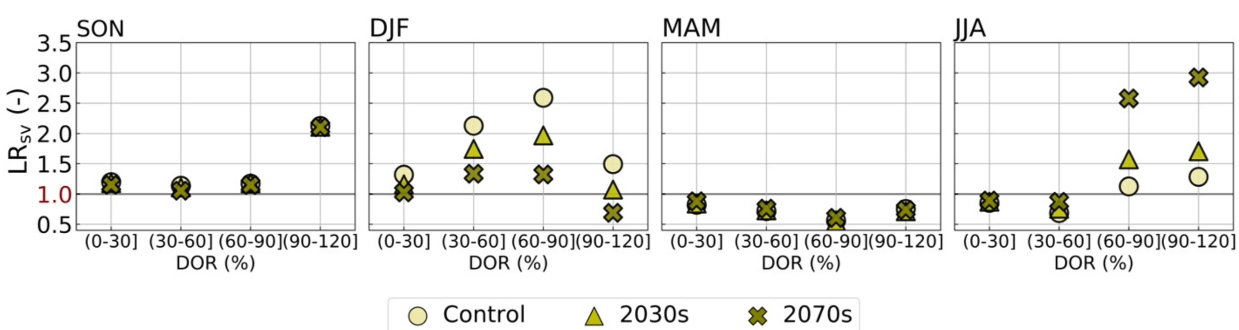


Fi

5. September-November (SON), December-February (DJF), March-May (MAM), and July-August (JJA) level of seasonal volume regulation (LRsv) across each period. LRsv is defined as the ratio of the regulated to unregulated seasonal volume. The figure shows the median LRsv from the 80-member ensemble. Ratios for each location have been grouped by the degree of upstream regulation (DOR) and averaged across each period. The lightest point shows the control period LRsv and the darkest point shows the 2070s LRsv.

In section 4.1.1, we showed that seasonal volumes are projected to change for both unregulated and regulated conditions; however, regulation effects on the magnitude and direction of change vary widely across seasons. Much of this can be explained by seasonally varying operations that alter flow timing and the seasonality of the annual hydrograph. Figure 5 shows the relationship between regulated and unregulated flow volumes and how these effects are projected to change in the future.

Spring (MAM) straddles the period of the strong snowmelt pulse which typically occurs late spring/early summer. Streamflow across the basin is primarily snowmelt driven and control period peak flows typically occur during the spring freshet (see Figure 1). In the spring, reservoirs begin refilling (storing large volumes of water) for spring flood risk management and LRsv (equation (2)) is less than 1 because regulated flow volumes are less than unregulated flow volumes. Stored spring volumes are later used to augment dry season low flows, and winter drafting of reservoirs increases flood storage space in preparation for the next spring freshet. As a result, control period LRsv is greater than 1 across autumn (SON), winter (DJF), and summer (JJA) for locations where DOR is greater than 60%.

By the 2070s, large changes in the LRsv occur in winter and summer when regulation effects on volume changes exhibit the strongest patterns (widespread dampening effects in winter and summer). Unregulated winter volumes are projected to increase significantly; however, as the system is operated to maintain flows and reservoir storage for the management of flood risk, regulated volume changes are relatively smaller and LRsv-values approaches unity. Unregulated summer volumes are projected to decrease. Summer system operations maintain low flow conditions and flow augmentation results in less change under regulation and LRsv-values that exceed 1 where DOR is large.

### 4.2 High Flow Extremes (Q50RP)

#### *4.2.1 Large Regulation Effects on Q50RP Flow Changes Occur at Headwater Tributary Sites Where DOR is Large*

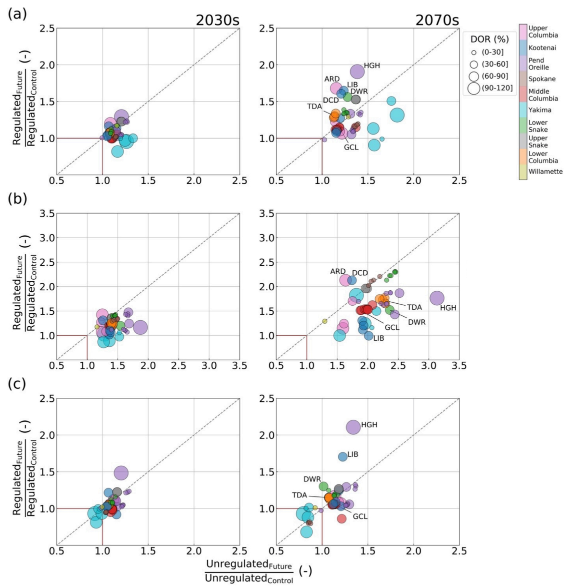


Figure 6. Annual (a), October-March (b), and April-September (c) 50-year return period peak flow ratios for unregulated conditions (x-axis) and regulated conditions (y-axis). Figure shows the median ratio across the 80-member ensemble. Points are colored by region and sized by the degree of upstream regulation (DOR). In the absence of regulation, points would fall on the dashed 1:1 line. The red box helps to identify the direction of change over time. Points within the red box indicate decreases in future Q50RP flows. Points outside of the box indicate increases in future Q50RP flows. Sites that show significant differences between regulated and unregulated conditions are annotated. Also annotated

are Grand Coulee (GCL) and The Dalles (TDA), located on the mainstem of the Middle Columbia and Lower Columbia, respectively.

Unregulated annual Q50RP flows are projected to increase by the 2070s across the domain (Figure 6a). The largest unregulated increases occur in the Yakima, Pend Oreille, Spokane, and Upper Snake subbasins (ordered from greatest increase to least). The effects of regulation vary spatially. Regulation significantly dampens changes in the Yakima and Spokane, tributaries where hydrologic regimes shift to rain-dominant by the 2070s. Regulation amplifies Q50RP changes for a number of locations across the domain. The greatest amplification effects occur downstream of headwater reservoirs in the Pend Oreille (Hungry Horse; HGH), Kootenai (Libby; LIB, Duncan; DCD), and Lower Snake (Dworshak; DWR). Strong regulation effects also occur at Arrow Lakes (ARD), a reservoir in the Upper Columbia. Amplification effects from these reservoirs diminish further downstream where dampening effects occur, particularly in the Kootenai and Upper Columbia (Figure S15 of Supporting Information).

We take a closer look at seasonal Q50RP changes to determine whether differences between unregulated and regulated conditions are driven by changes in the cool or warm season. During the cool season, unregulated Q50RP flows are projected to increase across the domain (Figure 6b) as a result of enhanced winter precipitation. Regulated Q50RP flows are also projected to increase; however, operations result in significantly less change where DOR is greater than 30%. Some of the largest dampening effects occur at Hungry Horse, Libby, and Dworshak. By the 2070s, regulation at Libby results in no cool-season change. At Arrow Lakes and Duncan, 2070s cool-season unregulated Q50RP flows exhibit increases of 63% and 74%, respectively; however, regulation amplifies these changes to 112% at both sites.

The warm season is a period when peak flows are driven by the spring freshet and climate change effects during this period are spatially variable (Figure 6c). Warm-season unregulated Q50RP flows are projected to decrease by the 2070s for regions that exhibit regime shifts to rain-dominance (Willamette, Spokane, and Yakima). Increases are projected for all other locations. Regulated changes generally follow unregulated changes. Exceptions occur at Hungry Horse, Libby, and Dworshak, where warm-season regulation results in greater relative change.

Arrow Lakes and Duncan remain snow dominant through the 2070s, yet regulation dampens the warm-season signal and amplifies the cool-season signal indicating that annual amplification effects are driven by cool-season increases in regulated flows. Hungry Horse, Libby, and Dworshak see amplification effects in the warm season, indicating that annual amplification effects are driven by warm-season increases in regulated flows.

#### *4.2.2 Level of Q50RP Regulation Shows Regulation Has Little Effect on Warm-Season Q50RP Changes*

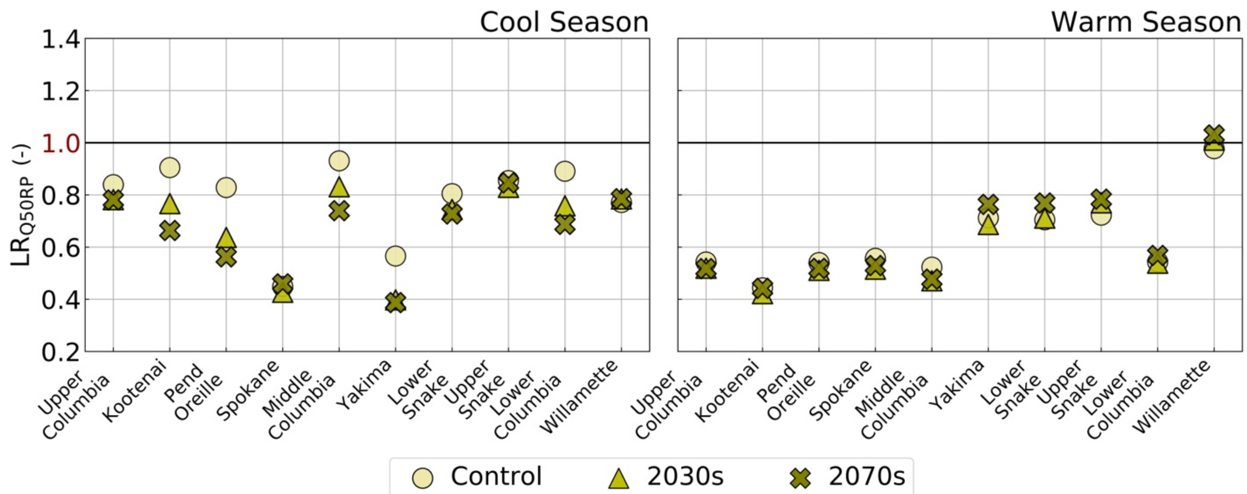


Figure 7. Seasonal level of regulation for the cool season (October-March) and warm season (April-September) where $LR_{Q50RP}$ (y-axis) is the level of regulation defined as the ratio of regulated to unregulated Q50RP. The figure shows the median $LR_{Q50RP}$ from the 80-member ensemble. Ratios at each location have been grouped by region and averaged across each period.

Figure 7 shows the level of Q50RP regulation ($LR_{Q50RP}$) (equation (3)) averaged by region for the cool season and the warm season. Across seasons and regions, $LR_{Q50RP}$ remains less than 1 in the future indicating that as the unregulated Q50RP increases the system still reduces unregulated high flow extremes in the future (also see Figure S17 of Supporting Information); however, regulated Q50RP will generally increase (Figure 6). Cool-season $LR_{Q50RP}$-values decrease in the future (regulated Q50RP is significantly less than unregulated Q50RP) indicating the system is largely reducing cool-season unregulated floods. In contrast, warm-season $LR_{Q50RP}$-values show little change or increases in the future (as unregulated Q50RP flows increase, regulated Q50RP flows also increase), indicating that regulation has little effect on the warm-season Q50RP signal and may be less effective at reducing unregulated high flow extremes in the future.

4.3 Low Flow Extremes (7Q10)

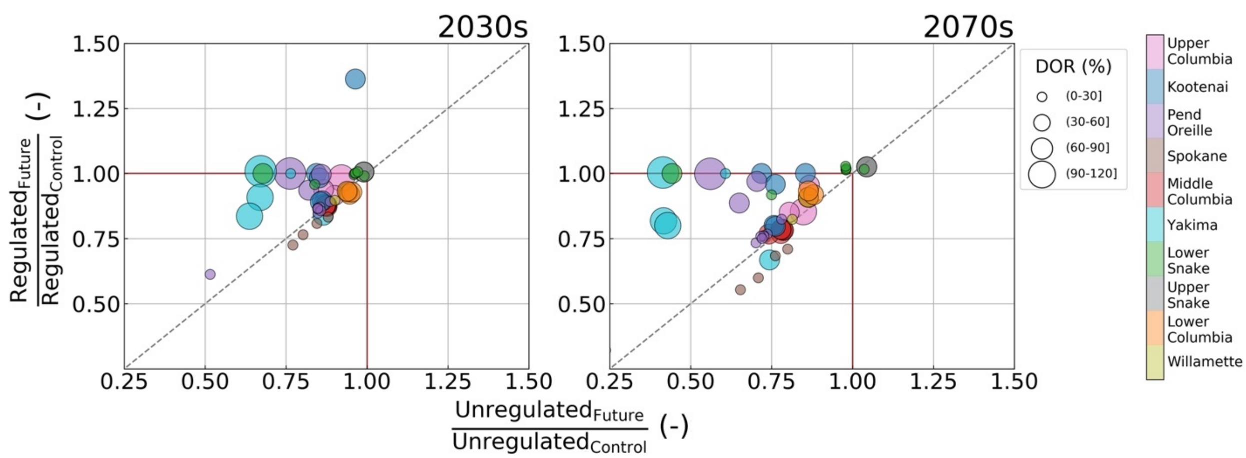


Figure 8. July-October 10-year return period 7-day average minimum flow (7Q10) ratios for unregulated conditions (x-axis) and regulated conditions (y-axis). Figure shows the median ratio across the 80-member ensemble. Points are colored by region and sized by the degree of upstream regulation (DOR). In the absence of regulation, points would fall on the dashed 1:1 line. The red box helps to identify the direction of change over time. Points within the red box indicate decreases in future 7Q10 flows. Points outside of the box indicate increases in future 7Q10 flows. For the 2070s, a single site in the Pend Oreille subbasin is not shown and exhibits a 76% decrease in 7Q10 flows.

Unregulated 7Q10 flows are projected to decrease by both the 2030s and the 2070s across most sites (Figure 8). By the 2070s, the largest decreases occur in the Pend Oreille, Yakima, and Lower Snake subbasins where regimes shift from snow-dominant to transient or transient to rain-dominant. Unregulated 7Q10 flows in the Yakima decrease by over 50%. Regulated changes generally follow unregulated changes. Exceptions occur in headwater tributaries of the Kootenai, Pend Oreille, Yakima, and Lower Snake subbasins where the high DOR reflects dry season flow augmentation. On the mainstem, where DOR is lower, regulated flows are more susceptible to the climate signal showing little to no difference from unregulated changes.

## 5 Discussion

Seasonally, regulation dampens winter and summer flow volume changes where DOR is greater than 30%. Unregulated seasonal volume changes are largest in winter, a period when precipitation is projected to increase the most and warmer temperatures result in more cool-season precipitation falling as rain rather than snow. All locations exhibit future increases in unregulated winter volumes and there is strong agreement across the ensemble in the direction of change (Table S3 of Supporting Information). Regulated winter volumes also increase across most sites, but water management operations result in significantly smaller relative changes. In the summer, warmer and drier conditions drive decreases in unregulated volumes, and, like winter, models agree on the direction of summer change (Table S5 of Supporting Information). Regulation generally reduces summer volume changes and sites with very large DOR exhibit increasing volumes due to large summer flow augmentation.

These results align with other studies that have investigated regulation effects on changing conditions in the Columbia River basin. Jones and Hammond (2020) investigated historical trends in inflows and outflows for large reservoirs across the basin and found that during the dry season, inflows to reservoirs decreased while outflows increased due to the effects of low flow augmentation. Zhou et al. (2018) examined regulation effects on the timing of climate signal emergence (defined by the timing of hydrologic regime shifts) across the western US. Regulation effects in the Columbia River basin showed high seasonal dependence and delayed the timing of climate signal emergence during winter and summer.

The seasonal dependence of regulation effects can be explained by seasonal water management operations and projected future hydroclimate. Seasonal reservoir storage and the delayed release of inflows alter streamflow timing. In the Columbia River basin, reservoirs store large snowmelt driven spring volumes that are later used to augment late summer/early autumn flows and are then released (drafted) throughout winter in preparation for the next spring freshet. This delayed release results in summer, autumn, and winter reservoir outflows that exceed unregulated flows (Figure 5). As unregulated summer volumes decrease in the future, reservoirs release more water to augment lower summer volumes resulting in a dampened summer climate signal and, also, reservoirs that are less full by winter. As unregulated winter volumes increase, less full reservoirs release less inflow to meet spring flood risk management objectives resulting in smaller relative change and a dampened winter signal.

The results for autumn and spring vary spatially. Unlike projections for the winter and summer, flow projections for the autumn and spring exhibit uncertainty in the direction of change across the ensemble (Tables S2 and S4 of Supporting Information) driven by large uncertainty in precipitation patterns (RMJOC, 2018). Nevertheless, results for autumn and spring can be explained by the seasonality of operations. For snow/transient subbasins that shift to transient/rain by the 2070s, regulated autumn volumes decrease where little to no unregulated change occurs. As snowpack decreases and summers become drier, large summer augmentation effects could result in less water stored in reservoirs by autumn and consequently, decreased autumn outflows. Spring regulation effects vary depending on hydroclimate and site-specific operational constraints. March through May straddles the onset of the spring refill period. As warming shifts snowmelt timing earlier, reservoirs that historically empty through late spring could experience an amplified spring signal if large volumes that occurred during reservoir refill shift earlier to periods of drafting.

Regulation results in dampening and amplification of high flow extreme changes and these effects exhibit high seasonal and spatial dependence. For most locations, winter regulation significantly reduces relative increases in cool-season extremes when unregulated high flow extremes are projected to increase the most as a result of enhanced precipitation; however, warm-season and annual changes are spatially variable. Unregulated annual Q50RP values are projected to increase across the domain (Figure 6a). This is in agreement with other studies that used the same unregulated flow dataset to investigate changes in future extremes (Chegwidden et al., 2020; Queen et al., 2019). Outflow from historically snow dominant headwater reservoirs where DOR is large exhibit amplification of annual Q50RP changes, but these effects generally diminish downstream where, in many cases, dampening occurs.

The phenomenon of regulated flows exhibiting greater sensitivity to climate change has been discussed before, although, not in the context of extreme flows. Zhou et al. (2018) found that some regulated basins in the Western US are projected to be more sensitive to the climate signal, experiencing earlier shifts in the hydrologic regime relative to unregulated conditions. They explain this phenomenon as the result of less variation in the seasonality of a "flattened-out" hydrograph under regulation. Small seasonal shifts in outflow from reservoirs during periods when streamflow is historically regulated can lead to greater relative change under regulation. For example, if a reservoir releases less water after a high flow extreme event in the past (historically low reservoir outflow after an unregulated high flow event) but releases more water after these events in the future, the changes under regulation can be large. At Hungry Horse (HGH), Libby (LIB), and Dworshak (DWR), high elevation headwater reservoirs in the Pend Oreille, Kootenai, and Lower Snake subbasins, respectively, hydrologic regimes shift from snow-dominant to transient or near-transient by the 2070s (Figure 2). Regulation for these locations reduces (flattens) the seasonality of the annual hydrograph (Figure 1). Operations at these sites result in significant dampening of cool-season extreme changes (Figure 6b) and amplification of warm-season changes (Figure 6c). Each of these reservoirs is operated for winter and spring flood risk management (RMJOC, 2020). In a transitional climate, large increases in the magnitude of unregulated winter flood events could result in difficulty in meeting spring draft and refill requirements and lead to higher reservoir outflows in the future and an amplified signal.

In contrast, sensitivity studies for rain-dominant basins in East Asia found that reservoir operations resulted in widespread dampening of high flow extreme changes (Dong et al., 2019; Wang et al., 2017; Yun et al., 2021). Wang et al. (2017) studied regulation effects in the Lancang-Mekong River basin and found that the largest attenuation effects occur in headwater basins where DOR is large and weaken downstream. They argue that stronger regulation effects occur at upstream reservoirs due to relatively smaller annual discharges. We show the largest amplification effects occur at historically snow-dominant headwater reservoirs with large DOR and generally diminish downstream where, in most cases, dampening occurs (Figure S15 of Supporting Information). These contrasting effects are likely due to historical regime patterns. The regulated flows used in this study result from seasonal operations based on current and historical water demands that do not change to account for large regime shifts from snow dominant. As streamflow timing shifts in the future, historically-based patterns of reservoir draft and refill result in geater outflow during periods when it was historically regulated. Amplification upstream and dampening downstream can be explained by the effects of operations. Headwater reservoirs will store more water during larger unregulated flood events thereby reducing the signal downstream. Water stored during these events is released after the events when downstream flood risk is reduced, which could locally lead to future increases in high flows but have less effect further downstream.

Although large changes in high flow extremes occur for both regulated and unregulated conditions, flood risk management operations continue to reduce unregulated floods into the future (Figure 7 and Figure S17 of Supporting Information). Increases in regulated high flow extremes do not necessarily indicate increased flooding downstream. This study identified these increases and linked them to higher reservoir outflows; however, did not examine the likelihood of high flows reaching levels where flood damages occur.

Unregulated July through October low flows are generally projected to decrease and the effects of regulation vary spatially. Significant dampening occurs in tributaries where DOR is large. High DOR locations have the highest augmentation effects in the future (Figure 5) and consequently, large regulation effects on the low flow extreme signal. Regulated flows on the mainstem are susceptible to the natural climate signal exhibiting little to no regulation effect on low flow changes.

Spatial patterns in the regulated 7Q10 response may be the result of spatially variable operational objectives. Dudley et al. (2020) compared 7-day low flow historical trends between unregulated and regulated gages across the US. In the western US, unregulated low flows exhibited a downward trend. Regulated low flows generally exhibited an upward trend indicating that reservoir operations mitigated climate change impacts on low flows; however, regulated trend results were mixed which they described as a likely consequence of diversity in regional climate and operational purpose. Large DOR occurs downstream of tributary and headwater reservoirs where annual discharge volumes are smaller relative to the mainstem. These regions could be more susceptible to low flow-associated risks (e.g., ecosystem vulnerability) and large DOR could indicate more operational flexibility to dampen large shifts in low flow extremes. DOR is smaller on the mainstem, and results could indicate less operational flexibility in the future to meet low flow storage targets during extreme events. Jones and Hammond (2020) showed that while water management in the Columbia River basin has historically adjusted to long-term downward trends in low flows, operational risks associated with the inability to meet seasonal flow targets increased during periods with lower than average flows.

Columbia River basin reservoir operations vary seasonally and serve multiple and sometimes competing system objectives. In the autumn, winter, and spring, reservoirs are primarily operated to provide storage for flood risk, hydropower, and ecological health. Summer flows and volumes are important for meeting hydropower, navigation, recreation, and irrigation demands (RMJOC, 2020). Climate change is projected to shift the hydrologic regime from snow-dominant to transient or rain-dominant, with large increases in unregulated winter volumes and decreases in summer volumes. Reservoir operations generally reduce these changes by storing larger inflows in the winter and augmenting more in the summer. High and low flow unregulated extreme events will be exacerbated under climate change. The patterns of seasonal reservoir operations result in dampened effects for cool-season high flow increases, but the regulated system exhibits sensitivity to high flow increases during the warm-season. Decreases in low flow extremes are dampened by regulation in tributaries but sensitivity on the mainstem could result from operations that are less flexible given historically-based objectives. The reservoir system's ability to meet competing operational objectives in the future may be strained by large shifts in seasonal hydrology; however, as streamflow timing shifts earlier in the water year, the operational patterns of seasonal storage (drafting to create flood space for the spring freshet and refill) could also shift, potentially reducing sensitivities. For example, adjustment of refill operations to accommodate shifts in snowmelt timing and volume could increase the likelihood of refill and the effectiveness of the system to store water to augment lower dry-season flows. The system may also encounter new competing objectives. An example of competing objectives is the increased frequency of bi-modal flood seasons. Storing inflows to reduce winter flooding could interfere with drafting reservoirs to create flood storage for the spring freshet.

This study examined the effects of regulation on climate change outcomes in the Columbia River basin; however, we attribute outcomes to broad basin characteristics across a large domain and results can be generalized for other regulated snow and transient basins. Large regime shifts in hydrologically diverse basins combined with seasonal and multi-objective reservoir operations result in regulated outcomes that vary widely across time and space. Considering the role of regulation in climate sensitivity analysis, particularly for basins that exhibit strong seasonality, is the first step in identifying adaptive management needs.

## 6 Limitations

The regulated flows examined in this study result from operating criteria based on the current operational constraints of the system. It is unlikely that seasonal operational patterns will remain static in the future with large shifts in seasonal hydrology. As climate and water demands shift, water management will need to adapt to changing conditions to continue meeting the multi-objectives of the system and operational patterns will need to change. Here we identified the effects of climate changed hydrology under current operating criteria and highlight the importance of considering reservoir operations in climate sensitivity analysis. While modeling the effects of modified operations is not within this scope, these findings will inform future work on adaptative management design for climate change.

We characterize outcomes by the medians of large ensembles of seasonal volume and extreme flow changes. The ensembles were driven by a diverse set of climate scenarios, statistical downscaling methods, and hydrologic model configurations that capture a wide range of uncertainty not examined in this paper for the sake of concisely describing key differences for several metrics important for water management. Furthermore, while rigorous model validation and bias-correction techniques were applied at each element of the modeling chain during dataset development (Chegwidden et al., 2018; RMJOC, 2018, 2020), there are uncertainties associated with each step in the process not addressed in this paper (Chegwidden et al., 2018, 2020; Queen et al., 2020; RMJOC, 2018, 2020; Rupp et al., 2021). Additional uncertainty was introduced by extrapolating extreme events from analytical distributions (LP3) fit to the unregulated and regulated empirical time series. As we report in the Supporting Information, two goodness of fit tests were performed on these analytical distributions and, generally, the LP3 curve provided robust estimates for both high and low flow extremes for most locations across the ensemble (Figures S3-S14 of Supporting Information). Some exceptions occurred for estimates at highly regulated headwater locations; however, despite these results there was strong correlation between the analytical and empirical distributions for a majority of ensemble members and the LP3 analytical fits provided a consistent framework for evaluating all locations.

## 7 Conclusions

Regulation modulates the seasonality of the annual hydrograph. The signature of regulation on streamflow patterns varies across time and across the basin. Reservoir operations result in significantly less change for winter and summer streamflow volumes at locations where DOR is large, but results for autumn and spring vary widely depending on local operational constraints and hydroclimate. Regulation effects on high flow extreme changes are also variable. Winter operations reduce changes in cool-season high flow extremes for locations where DOR is large. Annually and in the warm-season, regulation at historically snow-dominated headwater reservoirs amplifies the climate signal on high flows. These increases in flow reflect changes in reservoir release patterns as the system attempts to meet operational objectives under different hydrological conditions. In some cases, the operations developed for historical hydrological conditions are less effective in meeting these objectives as the hydrology changes. In many cases, not adjusting operations for streamflow timing and regime shifts results in greater relative high flow changes under regulation. Dry-season low flow extreme outcomes are dependent on location in the river network. On the mainstem, the regulated system exhibits sensitivity to low flow extremes following changes in unregulated low flows; however, for tributaries where upstream DOR is large, regulation significantly dampens low flow changes.

The reality of freshwater systems world-wide is that the majority are heavily fragmented by reservoirs (Grill et al., 2015). This study has shown that water resource infrastructure and reservoir operations are a constraint that can have large effects on climate outcomes, particularly in snow-dominant watersheds where large regime shifts challenge historically-based assumptions. These effects will have implications for managed freshwater systems and the future of water resources in regulated systems. By accounting for the role of regulation in climate sensitivity analysis, a more accurate characterization of climate outcomes will help inform where and how to adapt water management systems for a future climate.

Acknowledgments, Samples, and Data

The regulated and unregulated streamflow datasets used in this study were developed through a collaboration between the US Army Corps of Engineers, the Bureau of Reclamation, the Bonneville Power Administration, Oriana Chegwidden and Bart Nijssen with the University of Washington, and David Rupp and Philip Mote with Oregon State University. The authors of this study appreciate all collaborators who developed and shared the datasets to make this work possible. Jane Harrell was supported in part by a National Science Foundation Graduate Research Fellowship under Grant No. DGE-1762114. The unregulated streamflow projection data used in this study are available at https://doi.org/10.5281/zenodo.854763 (Chegwidden et al., 2017). The unregulated and regulated streamflow statistics presented in this paper are available at https://doi.org/10.5281/zenodo.5866731 (Harrell et al., 2022).

References

Arheimer, B., Donnelly, C., & Lindström, G. (2017). Regulation of snow-fed rivers affects flow regimes more than climate change. *Nature Communications*, *8*(1). https://doi.org/10.1038/s41467-017-00092-8

Barnes, C. A., Duxbury, A. C., & Morse, B.-A. (1972). Circulation and selected properties of the Columbia River effluent at sea. In A.T. Pruter and D.L. Alverson (Eds.), *The Columbia River Estuary and Adjacent Ocean Waters*. Seattle, WA: University of Washington Press.

Barnett, T. P., Adam, J. C., & Lettenmaier, D. P. (2005). Potential impacts of a warming climate on water availability in snow-dominated regions. *Nature, 438(7066)*, 303–309. https://doi.org/10.1038/nature04141

Bonneville Power Administration. (2011). 2010 level modified streamflow: 1928-2008. Portland, OR: Bonneville Power Administration. Retrieved May 15$^{th}$ 2021 from https://www.bpa.gov/-/media/Aep/power/historical-streamflow-reports/

Bureau of Reclamation. (2009). Naturalized and modified flows of the Deschutes River Basin. Boise, ID: Bureau of Reclamation, Pacific Northwest Regional Office.

Bureau of Reclamation. (2010a). Modified and naturalized flows of the Snake River Basin above Brownlee Reservoir. Boise, ID: Bureau of Reclamation, Pacific Northwest Regional Office.

Bureau of Reclamation. (2010b). Naturalized and modified flows of the Yakima River Basin, Columbia River Tributary, Washington. Yakima, WA: Bureau of Reclamation, Columbia-Cascades Area Office.

Bureau of Reclamation. (2011). Climate and Hydrology Datasets for Use in the RMJOC Agencies' Longer-Term Planning Studies: Part II – Reservoir Operations Assessment for Reclamation Tributary Basins. Boise, ID: Bureau of Reclmation, Pacific Northwest Regional Office. Retrieved from https://www.usbr.gov/pn/climate/planning/reports/part2.pdf

Bureau of Reclamation. (2016). Columbia River Basin: climate impact assessment. Boise, ID: Bureau of Reclamation, Pacific Northwest Regional Office.

Chegwidden, O. S., Nijssen, B., Rupp, D. E., & Mote, P. W. (2017). Hydrologic response of the Columbia River System to climate change [Dataset]. Zenodo. https://doi.org/10.5281/zenodo.854763.

Chegwidden, O. S., Nijssen, B., Rupp, D. E., Arnold, J. R., Clark, M. P., Hamman, J. J., et al. (2019). How do modeling decisions affect the spread among hydrologic climate change projections? Exploring a large ensemble of simulations across a diversity of hydroclimates. *Earth's Future, 7(6)*, 623–637. https://doi.org/10.1029/2018EF001047

Chegwidden, O. S., Rupp, D. E., & Nijssen, B. (2020). Climate change alters flood magnitudes and mechanisms in climatically-diverse headwaters across the northwestern United States. *Environmental Research Letters, 15(9).* https://doi.org/10.1088/1748-9326/ab986f

Dong, N., Yu, Z., Gu, H., Yang, C., Yang, M., Wei, J., et al. (2019). Climate-induced hydrological impact mitigated by a high-density reservoir network in the Poyang Lake Basin. *Journal of Hydrology, 579(June)*, 124148. https://doi.org/10.1016/j.jhydrol.2019.124148

Dudley, R. W., Hirsch, R. M., Archfield, S. A., Blum, A. G., & Renard, B. (2020). Low streamflow trends at human-impacted and reference basins in the United States. *Journal of Hydrology*, *580(April 2019)*, 124254. https://doi.org/10.1016/j.jhydrol.2019.124254

Dynesius, M., & Nilsson, C. (1994). Fragmentation and flow regulation of river systems in the northern third of the world. *Science, 266(5186),* 753–762. https://doi.org/10.1126/science.266.5186.753

Elsner, M. M., Cuo, L., Voisin, N., Deems, J. S., Hamlet, A. F., Vano, J. A., et al. (2010). Implications of 21st century climate change for the hydrology of Washington State. *Climatic Change, 102(1–2)*, 225–260. https://doi.org/10.1007/s10584-010-9855-0

England, J.F., Jr., Cohn, T.A., Faber, B.A., Stedinger, J.R., Thomas, W.O., Jr., Veilleux, A.G., Kiang, J.E., and Mason, R.R., J. (2018). Guidelines for determining flood flow frequency Bulletin 17C Book 4, hydrologic analysis and interpretation techniques and methods 4-B5. Retrieved from https://pubs.usgs.gov/tm/04/b05/tm4b5.pdf

Esri. (2009). *World Physical Map.* Retrieved from https://services.arcgisonline.com/ArcGIS/rest/services/Wor

Esri. (2011). *World Light Gray Reference.* Retrieved from https://services.arcgisonline.com/ArcGIS/rest/servi

Frans, C., Istanbulluoglu, E., Lettenmaier, D. P., Fountain, A. G., & Riedel, J. (2018). Glacier recession and the response of summer streamflow in the Pacific Northwest United States, 1960–2099. *Water Resources Research, 54(9)*, 6202–6225. https://doi.org/10.1029/2017WR021764

Fritze, H., Stewart, I. T., & Pebesma, E. (2011). Shifts in Western North American snowmelt runoff regimes for the recent warm decades. *Journal of Hydrometeorology, 12(5)*, 989–1006. https://doi.org/10.1175/2011JHM1360.1

Gergel, D. R., Nijssen, B., Abatzoglou, J. T., Lettenmaier, D. P., & Stumbaugh, M. R. (2017). Effects of climate change on snowpack and fire potential in the western USA. *Climatic Change, 141(2)*, 287–299. https://doi.org/10.1007/s10584-017-1899-y

Grill, G., Lehner, B., Thieme, M., Geenen, B., Tickner, D., Antonelli, F., et al. (2019). Mapping the world's free-flowing rivers. *Nature, 569(7755)*, 215–221. https://doi.org/10.1038/s41586-019-1111-9

Hamlet, A. F., & Lettenmaier, D. P. (2007). Effects of 20th century warming and climate variability on flood risk in the western U.S. *Water Resources Research, 43(6)*, 1–17. https://doi.org/10.1029/2006WR005099

Hamlet, A. F., Lee, S. Y., Mickelson, K. E. B., & Elsner, M. M. (2010). Effects of projected climate change on energy supply and demand in the Pacific Northwest and Washington State. *Climatic Change, 102(1–2)*, 103–128. https://doi.org/10.1007/s10584-010-9857-y

Harrell, J., Nijssen, B., & Frans. C. (2022). Supporting data for: Where and when does streamflow regulation significantly affect climate outcomes in the Columbia River Basin? [Dataset]. Zenodo. https://doi.org/10.5281/zenodo.5866731.

IPCC. (2014). Climate change 2014 synthesis report summary chapter for policymakers. *IPCC, 31.* https://doi.org/10.1017/CBO9781107415324

Jones, J. A., & Hammond, J. C. (2020). River management response to multidecade changes in timing of reservoir inflows, Columbia River Basin, USA. *Hydrological Processes, 34(25)*, 4814–4830. https://doi.org/10.1002/hyp.13910

Kammerer, J. C. (1990). Largest rivers in the United States. United Stated Geological Survey, Department of the Interior. Retrieved from http://pubs.usgs.gov/of/1987/ofr87-242/pdf/ofr87242.pdf

Labadie, J. W. (2006). MODSIM: Decision support system for integrated river basin management. In *3rd International Congress on Environmental Modelling and Software,* Burlington, VT. Retrieved from https://scholarsarchive.byu.edu/iemssconference/2006/all/242

Leavesley, G. H., Lichty, R. W., Troutman, B. M., & Saindon, L. G. (1983). Precipitation-runoff modeling system—User's manual. U.S. Geological Survey

Water-Resources Investigations Report, 83(4238), 207.

Lee, S. Y., Hamlet, A. F., & Grossman, E. E. (2016). Impacts of climate change on regulated streamflow, hydrologic extremes, hydropower production, and sediment discharge in the Skagit River Basin. *Northwest Science, 90(1)*, 23–43. https://doi.org/10.3955/046.090.0104

Lee, S., Won, J., Binder, L. W., & Lott, F. (2018). Effect of climate change on flooding in King County rivers: using new regional climate model simulations to quantify changes in flood. Seattle, WA: Climate Impacts Group, University of Washington. Retrieved from https://cig.uw.edu/publications/effect-of-climate-change-on-flooding-in-king-county-rivers-using-new-regional-climate-model-simulations-to-quantify-changes-in-flood-risk/

Lehner, B., Liermann, C. R., Revenga, C., Vörömsmarty, C., Fekete, B., Crouzet, P., et al. (2011). High-resolution mapping of the world's reservoirs and dams for sustainable river-flow management. *Frontiers in Ecology and the Environment, 9(9)*, 494–502. https://doi.org/10.1890/100125

Leppi, J. C., DeLuca, T. H., Harrar, S. W., & Running, S. W. (2012). Impacts of climate change on August stream discharge in the Central-Rocky Mountains. *Climatic Change, 112(3–4)*, 997–1014. https://doi.org/10.1007/s10584-011-0235-1

Li, H., Wigmosta, M. S., Wu, H., Huang, M., Ke, Y., Coleman, A. M., & Leung, L. R. (2013). A physically based runoff routing model for land surface and earth system models. *Journal of Hydrometeorology, 14(3)*, 808–828. https://doi.org/10.1175/JHM-D-12-015.1

Liang, X., Lettenmaier, D. P., Wood, E. F., & Burges, S. J. (1994). A simple hydrologically based model of land surface water and energy fluxes for general circulation models. *Journal of Geophysical Research, 99(D7)*. https://doi.org/10.1029/94jd00483

Lute, A. C., Abatzoglou, J. T., & Hegewisch, K. C. (2015). Projected changes in snowfall extremes and interannual variability of snowfall in the western United States. *Water Resources Research*. https://doi.org/10.1002/2014WR016267

Mantua, N., Tohver, I., & Hamlet, A. (2010). Climate change impacts on streamflow extremes and summertime stream temperature and their possible consequences for freshwater salmon habitat in Washington State. *Climatic Change, 102(1–2)*, 187–223. https://doi.org/10.1007/s10584-010-9845-2

May C., Luce, C., Casola, J., Chang, M., Cuhaciyan, J., Dalton, M., et al. (2018). Chapter 24: Northwest. In D.R. Reidmiller, C.W. Avery, D.R. Easterling, K.E. Kunkel, K.L.M. Lewis, T.K. Maycock, and B.C. Stewart (Eds.), *Impacts, Risks, and Adaptation in the United States: Fourth National Climate Assessment, Volume II* (1036–1100). Washington D.C., USA: US Global Change Research Program. https://doi.org/10.7930/NCA4.2018.CH24

Moore, R. D., Pelto, B., Menounos, B., & Hutchinson, D. (2020). Detecting the Effects of Sustained Glacier Wastage on Streamflow in Variably Glacierized Catchments. *Frontiers in Earth Science, 8(May).* https://doi.org/10.3389/feart.2020.00136

Mote, P. W., Li, S., Lettenmaier, D. P., Xiao, M., & Engel, R. (2018). Dramatic declines in snowpack in the western US. *Npj Climate and Atmospheric Science*, *1*(1). https://doi.org/10.1038/s41612-018-0012-1

Musselman, K. N., Lehner, F., Ikeda, K., Clark, M. P., Prein, A. F., Liu, C., et al. (2018). Projected increases and shifts in rain-on-snow flood risk over western North America. *Nature Climate Change, 8(9)*, 808–812. https://doi.org/10.1038/s41558-018-0236-4

Payne, J., Wood, A., & Hamlet, A. (2004). Mitigating the effects of climate change on the water resources of the Columbia River basin. *Climatic Change, 62(1–3)*, 233–256. https://doi.org/10.1023/B:CLIM.0000013694.18154.d6

Queen, L. E., Mote, P. W., Rupp, D. E., Chegwidden, O., & Nijssen, B. (2021). Ubiquitous increases in flood magnitude in the Columbia River basin under climate change. *Hydrology and Earth System Sciences, 25(1)*, 257–272. https://doi.org/10.5194/hess-25-257-2021

Reidmiller, D.R., Avery, C.W., Easterling, D.R., Kunkel, K.E., Lewis, K.L.M., Maycock, T.K., and Stewart, B.C. (2018). Impacts, risks, and adaptation in the United States: fourth national climate assessment, volume II. Washington D.C., USA: US Global Change Research Program. https://doi.org/10.7930/NCA4.2018

RMJOC (River Management Joint Operating Committee). (2018). Climate and hydrology datasets for RMJOC long-term planning studies: Second Edition (RMJOC-II) Part I: Hydroclimate projections and analyses. Portland, OR: River Management Joint Operating Committee. Retrieved from https://usace.contentdm.oclc.org/digital/collection/p266001coll1/id/10562/rec/3

RMJOC (River Management Joint Operating Committee). (2020). Climate and hydrology datasets for RMJOC long-term planning studies: Second Edition (RMJOC-II) Part II: Columbia River reservoir regulation and operations-modeling and analyses. Portland, OR: River Management Joint Operating. Retrieved from https://usace.contentdm.oclc.org/digital/collection/p266001coll1/id/9936/rec/3

Rupp, D. E., Abatzoglou, J. T., & Mote, P. W. (2017). Projections of 21st century climate of the Columbia River Basin. *Climate Dynamics, 49(5–6)*, 1783–1799. https://doi.org/10.1007/s00382-016-3418-7

Rupp, D. E., Chegwidden, O. S., Nijssen, B., & Clark, M. P. (2021). Changing river network synchrony modulates projected increases in high flows. *Water Resources Research*, *2018*, 1–17. https://doi.org/10.1029/2020wr028713

Salathé, E. P., Hamlet, A. F., Mass, C. F., Lee, S. Y., Stumbaugh, M., & Steed, R. (2014). Estimates of twenty-first-century flood risk in the Pacific Northwest based on regional climate model simulations. *Journal of Hydrometeorology, 15(5)*, 1881–1899. https://doi.org/10.1175/JHM-D-13-0137.1

Singh, N. K., & Basu, N. B. (2022). The human factor in seasonal streamflows across natural and managed watersheds of North America. *Nature Sustainability*. https://doi.org/10.1038/s41893-022-00848-1

Stedinger, J.R., Vogel, R.M., & Foufoula-Georgiou, E. (1993). Frequency analysis of extreme events. In D.R. Maidment (Ed.), *Handbook of Hydrology* (18.1-18.6).

Stern, C.V. (2020). Columbia river treaty review (R43287). Congressional Research Service. Retrieved from https://crsreports.congress.gov/product/pdf/R/R43287/23

Stewart, I. T., Cayan, D. R., & Dettinger, M. D. (2005). Changes toward earlier streamflow timing across western North America. *Journal of Climate, 18(8)*, 1136–1155. https://doi.org/10.1175/JCLI3321.1

Tohver, I. M., Hamlet, A. F., & Lee, S. Y. (2014). Impacts of 21st-century climate change on hydrologic extremes in the Pacific Northwest region of North America. *Journal of the American Water Resources Association, 50(6)*, 1461–1476. https://doi.org/10.1111/jawr.12199

USACE (US Army Corps of Engineers) (2013). HEC-ResSim Reservoir System Simulation User's Manual Version 3.1, (May), 556. Davis, CA: US Army Corps of Engineers Institute for Water Resources Hydrologic Engineering Center.

USACE (US Army Corps of Engineers) (2020). Columbia River System Operations Environmental Impact Statement Record of Decision. Portland, OR: Northwest Division US Army Corps of Engineers. Retrieved from https://www.nwd.usace.army.mil/CRSO/Final-EIS/

Vano, J. (2015). Seasonal hydrologic responses to climate change in the Pacific Northwest. *Water Resources Research, 51*, 1959–1976. https://doi.org/10.1002/2014WR015909.Received

Voisin, N., Li, H., Ward, D., Huang, M., Wigmosta, M., & Leung, L. R. (2013). On an improved sub-regional water resources management representation for integration into earth system models. *Hydrology and Earth System Sciences Discussions, 10(3)*, 3501–3540. https://doi.org/10.5194/hessd-10-3501-2013

Wang, W., Lu, H., Ruby Leung, L., Li, H. Y., Zhao, J., Tian, F., et al. (2017). Dam construction in Lancang-Mekong River Basin could mitigate future flood risk From warming-induced intensified rainfall. *Geophysical Research Letters, 44(20)*, 10,378-10,386. https://doi.org/10.1002/2017GL075037

Warner, M. D., & Mass, C. F. (2017). Changes in the climatology, structure, and seasonality of northeast pacific atmospheric rivers in CMIP5 climate simulations. *Journal of Hydrometeorology, 18(8)*, 2131–2141. https://doi.org/10.1175/JHM-D-16-0200.1

Wood, A. W., Leung, L. R., Sridhar, V., & Lettenmaier, D. P. (2004). Hydrologic implications of dynamical and statistical approaches to downscaling climate model outputs. *Climatic Change, 62(1–3)*, 189–216. https://doi.org/10.1023/B:CLIM.0000013685.99609.9e

Yun, X., Tang, Q., Li, J., Lu, H., Zhang, L., & Chen, D. (2021). Can reservoir regulation mitigate future climate change induced hydrological extremes in the Lancang-Mekong River Basin? *Science of the Total Environment, 785*, 147322. https://doi.org/10.1016/j.scitotenv.2021.147322

Zagona, E., Nowak, K., Rajagopalan, B., Carly, J., & Prairie, J. (2010). Riverware's integrated modeling and analysis tools for long-term planning under uncertainty. In *Proceedings of the Fourth Federal Interagency Hydrologic Modeling Conference*, Las Vegas, NV. Retrieved from https://www.colorado.edu/cadswes/sites/default/files/attached-files/10f_zagonanowak_03_01_10.pdf

Zhou, T., Voisin, N., Lenga, G., Huang, M., & Kraucunas, I. (2018). Sensitivity of regulated flow regimes to climate change in the western United States. *Journal of Hydrometeorology, 19(3)*, 499–515. https://doi.org/10.1175/JHM-D-17-0095.1

References From the Supporting Information

Chowdhury, J. U., & Stedinger, J. R. (1991). Confidence interval for design floods with estimated skew coefficient. *Journal of Hydraulic Engineering, 117(7)*, 811–831. https://doi.org/10.1061/(ASCE)0733-9429(1991)117:7(811)

Cohn, T. A., England, J. F., Berenbrock, C. E., Mason, R. R., Stedinger, J. R., & Lamontagne, J. R. (2013). A generalized Grubbs-Beck test statistic for detecting multiple potentially influential low outliers in flood series. *Water Resources Research, 49(8)*, 5047–5058. https://doi.org/10.1002/wrcr.20392

England, J.F., Jr. & Cohn, T.A. (2019). PeakfqSA software. Retrieved from https://sites.google.com/a/alumni.colostate.edu/jengland/bulletin-17c#Software

Helsel, D. R., Hirsch, R. M., Ryberg, K. R., Archfield, S. A., & Gilroy, E. J. (2020). Statistical methods in water resources: techniques and methods 4-A3. Reston, VA: US Geological Survey. https://doi.org/10.3133/tm4A3

Salas, J. D., Kroll, C. N., Cancelliere, A., Fernández, B., Raynal, J. A., & Lee, D. R. (2019). Low flows and droughts. In R.S.V. Teegavarapu, J.D. Salas, J.R. Stedinger (Eds.), *Statistical Analysis of Hydrologic Variables*, (269–332). https://doi.org/10.1061/9780784415177.ch08

Stedinger, J.R., Griffis, V.W. (2008). Flood frequency analysis in the United States: time to update. *Journal of Hydrologic Engineering, 13(4)*, 199-204. https://doi.org/10.1061/(ASCE)1084-0699(2008)13:4(199)

Stedinger, J.R., Vogel, R.M., & Foufoula-Georgiou, E. (1993). Frequency analysis of extreme events. In D.R. Maidment (Ed.), *Handbook of Hydrology* (18.1-

18.6).

Veilleux, A.G., Cohn, T.A., Flynn, K.M., Mason, R.R., Jr., & Hummel, P.R., (2014). Estimating magnitude and frequency of floods using the PeakFQ 7.0 program: U.S. Geological Survey fact sheet 2013-3108. https://dx.doi.org/10.3133/fs20133108

AGU PUBLICATIONS

*Water Resources Research*

Supporting Information for

**Where and When Does Streamflow Regulation Significantly Affect Climate Change Outcomes in the Columbia River Basin?**

[1]Jane Harrell, [1]Bart Nijssen, [2]Chris Frans

[1]Department of Civil and Environmental Engineering, University of Washington, Seattle, WA, USA

[2]Seattle District, U.S. Army Corps of Engineers, Seattle, WA, USA

**Contents of this file**

Text S1 to S3
Figure S1 to S17
Table S1 to S5

**Text S1. High Flow Frequency Methods**

The Log Pearson Type III (LP3) distribution with the Expected Moments Algorithm (Stedinger and Griffis, 2008) method was used to fit distribution curves to maximum time series. Distributions were computed using PeakfqSA (England and Cohn, 2019), a stand-alone version of the Unites States Geological Survey (USGS) Peakfq flood frequency software (Veilleux, et al. 2014). PeakfqSA configuration file options were set to use the station (at-site) skew, the Multiple Grubbs Beck test (Cohn et al., 2013) to detect and adjust for low outliers, and the plotting position

$$p_{i:n} = \frac{i - \alpha}{n + 1 - 2\alpha} \tag{1}$$

where $\alpha = 0.4$ and $n$ is the sample size of the data.

**Text S2. Low Flow Frequency Methods**

The LP3 distribution with the method of moments was used to describe annual July-October 7-day average minimums. Calculation of the distribution and confidence intervals followed methods presented by Chowdhury and Stedinger (1991) and Stedinger et al. (1993). If $X_p$ is the $p^{th}$ quantile of the LP3 distribution, then

$$X_p = 10^{(\mu_y - K_p \sigma_y)}, \tag{2}$$

where $\mu_y$ and $\sigma_y$ are the mean and standard deviation of the log-transformed sample $y$, respectively. $K_p$ is approximated by the Wilson-Hilferty transformation.

$$K_p \approx \frac{2}{\gamma_m}\left(1+\frac{\gamma_y z_p}{6}-\frac{\gamma_y^2}{36}\right)^3-\frac{2}{\gamma}, \tag{3}$$

where $\gamma_y$ is the skew of the log-transformed sample and $z_p$ is the $p^{th}$ quantile of the standard normal distribution.

For each LP3 fit, we calculated the 90% confidence bounds $CI_{90}$,

$$CI_{90} = X_p \pm \eta\left(\zeta_{\alpha,p} - z_p\right)\sigma, \tag{4}$$

where $\sigma$ is the standard deviation of the sample, and $z_p$ is the $p^{th}$ quantile of the standard normal distribution. $\zeta_{0.5,p}$ is the 5$^{\text{th}}$ percentile of the noncentral $t$-distribution.

$$\zeta_{0.5,p} \approx \frac{z_p + z_{0.5}\sqrt{\frac{1}{n}+\frac{z_p^2}{2(n-1)}-\frac{z_{0.5}^2}{2n(n-1)}}}{1-\frac{z_{0.5}^2}{2(n-1)}}, \tag{5}$$

where $n$ is the sample size of the data and $z_{0.5}$ is the 5$^{\text{th}}$ quantile of the standard normal distribution. $z$ values were determined using the Python's `scipy.stats.norm.ppf` module. $\eta$ is a scaling factor to extend confidence intervals for normal quantiles to the LP3 distribution.

$$\eta \cong \sqrt{\frac{1+\gamma K_p+\frac{1}{2}\left(1+\frac{3}{4}\gamma^2\right)K_p^2}{1+\frac{1}{2}z_p^2}}. \tag{6}$$

Time series of low flows may exhibit autocorrelation due to groundwater dependence. Autocorrelation violates the assumption that our data are independent and, therefore, our goodness of fit. We tested for autocorrelation using Pearson's lag-1 correlation coefficient

$$r = \frac{\sum_{i=1}^{n-1}(x_i-\bar{x})(x_{i+1}-\bar{x})}{\sum_{i=1}^{n}(x_i-\bar{x})^2}, \tag{7}$$

where $n$ is the sample size. The sample was considered autocorrelated if $r > 0.3$. $r$ was calculated using Python's `scipy.stats.pearsonr` module. If autocorrelation was detected, we used the effective sample size (Dingman, 2015) to calculate confidence intervals by replacing $n$ in equation (6) with

$$n_{eff} = n\left(\frac{1-r}{1+r}\right). \tag{8}$$

Samples with zero-flows required truncation before log-transformation. We fit the LP3 curve to truncated samples and adjusted the probabilities to account for zero-flows using methods described by Salas et al. (2019). The probability $q$ that a given 7 day-minimum $X$ is less than or equal to $x_q$ is

$$P\left(X \leq x_q\right) = F\left(x_q\right) = q. \tag{9}$$

If a truncated sample has some number $n_o$ of zero values, an estimator of the probability of zero flow is

$$\hat{q}_0 = P(X = 0) = \frac{n_o}{n} \tag{10}$$

which can be used to adjust the probability $q$,

$$q_T = \frac{q - \hat{q}_0}{1 - \hat{q}_0}. \tag{11}$$

If after truncation and probability adjustments, the distribution did not contain the probability of interest (in our case, the 0.1 percentile corresponding to a 10-year return period), we fit the low flow frequency curve non-parametrically. Non-parametric confidence intervals were computed using the binomial distribution as described by Helsel et al. (2020). We also used non-parametric methods to fit the distribution if more than 10% of the sample fell outside of the LP3 confidence bounds.

**Text S3. Log Pearson Type III Goodness of Fit Tests**

The Kolmogorov-Smirnov (KS) and probability plot correlation coefficient (PPCC) goodness of fit tests (Stedinger et al., 1993) were performed to test the suitability of the LP3 analytical curves for fitting the unregulated and regulated high and low flow extreme time series. The KS tests evaluates whether the analytical estimates are drawn from the same population distribution as the empirical sample at the 90% confidence level by measuring the maximum difference between the analytical and empirical cumulative frequency curves. If the maximum difference is less than the KS test statistic $D$ (equation (12)) then we accept the null hypothesis that the two samples come from the same population distribution at the 90% confidence level. The test statistic $D$ is calculated as

$$D = 1.358\sqrt{\frac{n+m}{nm}} \tag{12}$$

where *n* is the sample size of the empirical sample and *m* is the sample size of the analytical sample. In our case, $n$ is 30 and $m$ is 41. We accept the null hypothesis if the maximum difference is less than the KS test statistic $D$ value of 0.326.

The PPCC measures the linearity of the probability plot. If the empirical sample is drawn from the analytical distribution, the probability plot of ordered empirical data $x_i$ versus the corresponding estimated probability $w_i$ should appear linear and the correlation coefficient $r$ (equation (13)) should be near 1.

$$r = \frac{\sum(x_i - \bar{x})(w_i - \bar{w})}{[\sum(x_i - \bar{x})^2 \sum(w_i - \bar{w})^2]^{0.5}} \qquad (13)$$

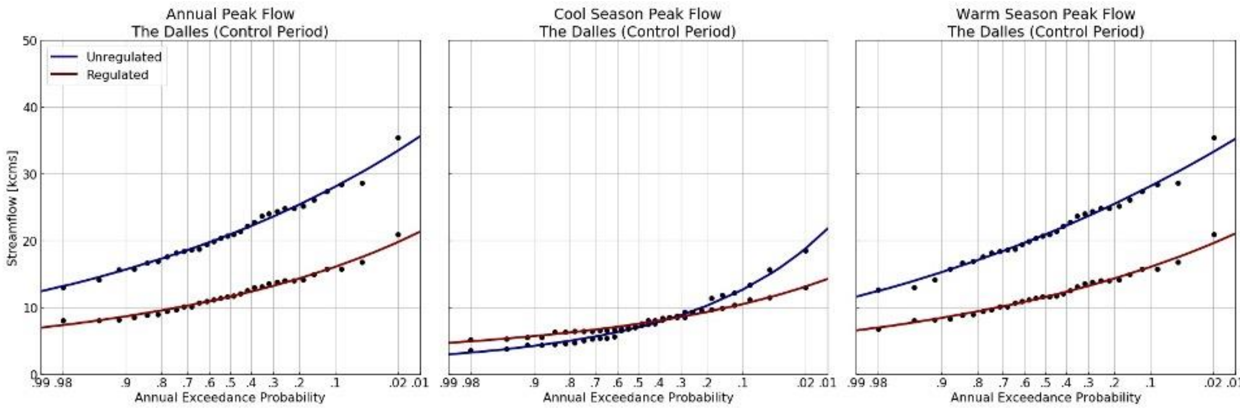


**Figure S1.** LP3 analytical fits for annual, cool season (October-March), and warm season (April-September) peak flows at The Dalles for a single ensemble member for the control period (1976-2005). Unregulated curves are shown in blue. Regulated curves are shown in red.

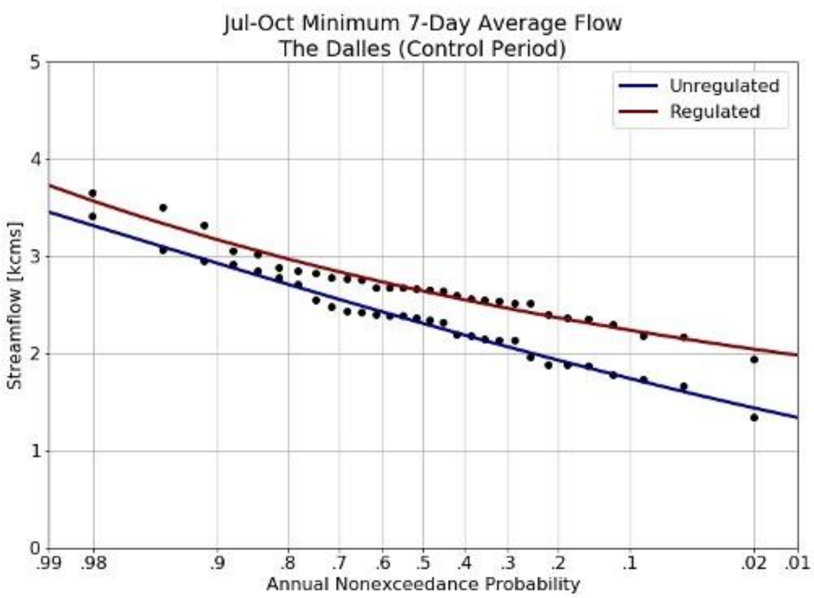


**Figure S2.** LP3 analytical fits annual minimum July-October 7-day average flows at The Dalles (TDA) for a single ensemble member for the control period (1976-2005). Unregulated curves are shown in blue. Regulated curves are shown in red.

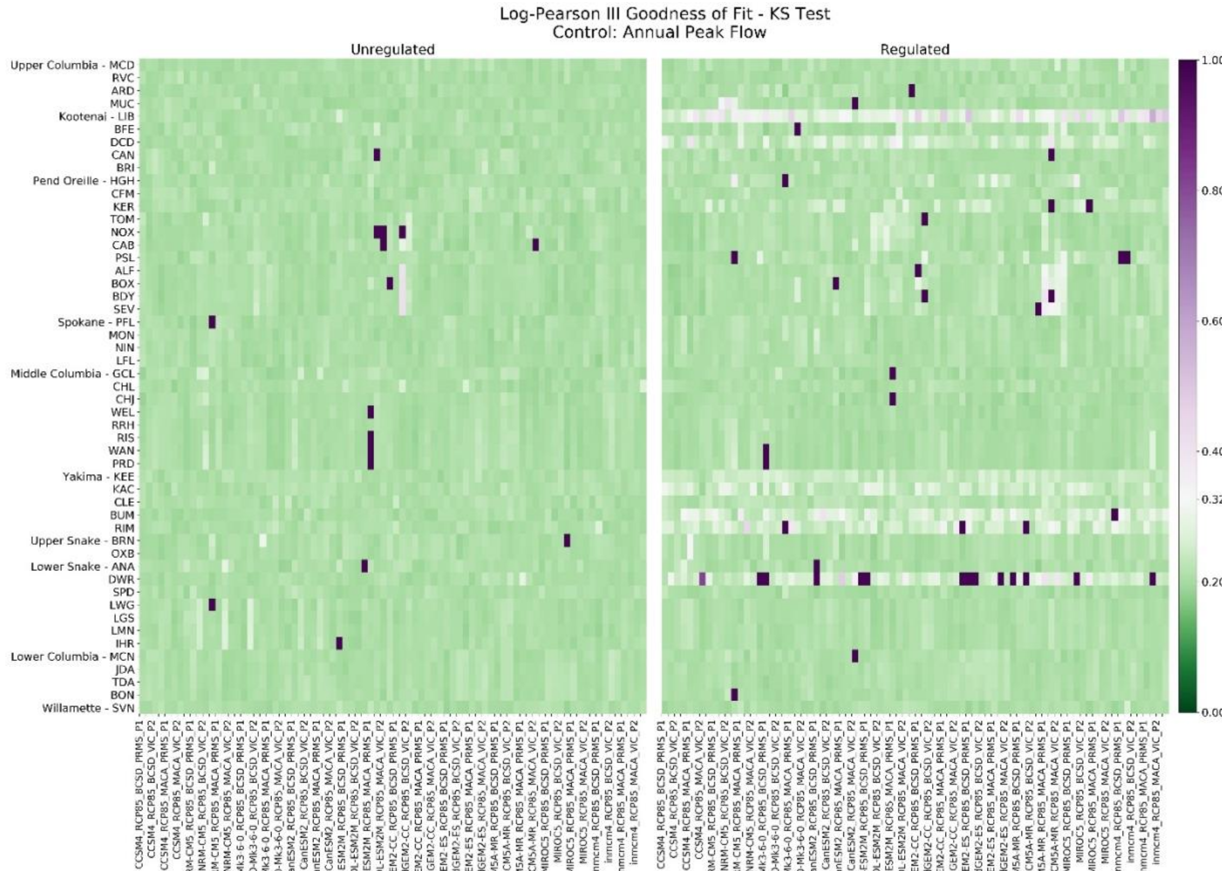


**Figure S3.** KS LP3 goodness of fit test results for control period annual peak flows for each ensemble member and each site included in the daily analysis. Test results are shown for unregulated analytical estimates (left) and regulated analytical estimates (right) and all 80 ensemble members (x-axis); however, only every other ensemble member is labelled. We accept the null hypothesis that the empirical and analytical populations are drawn from the same distributions if the maximum difference is less than the KS test statistic 0.326.

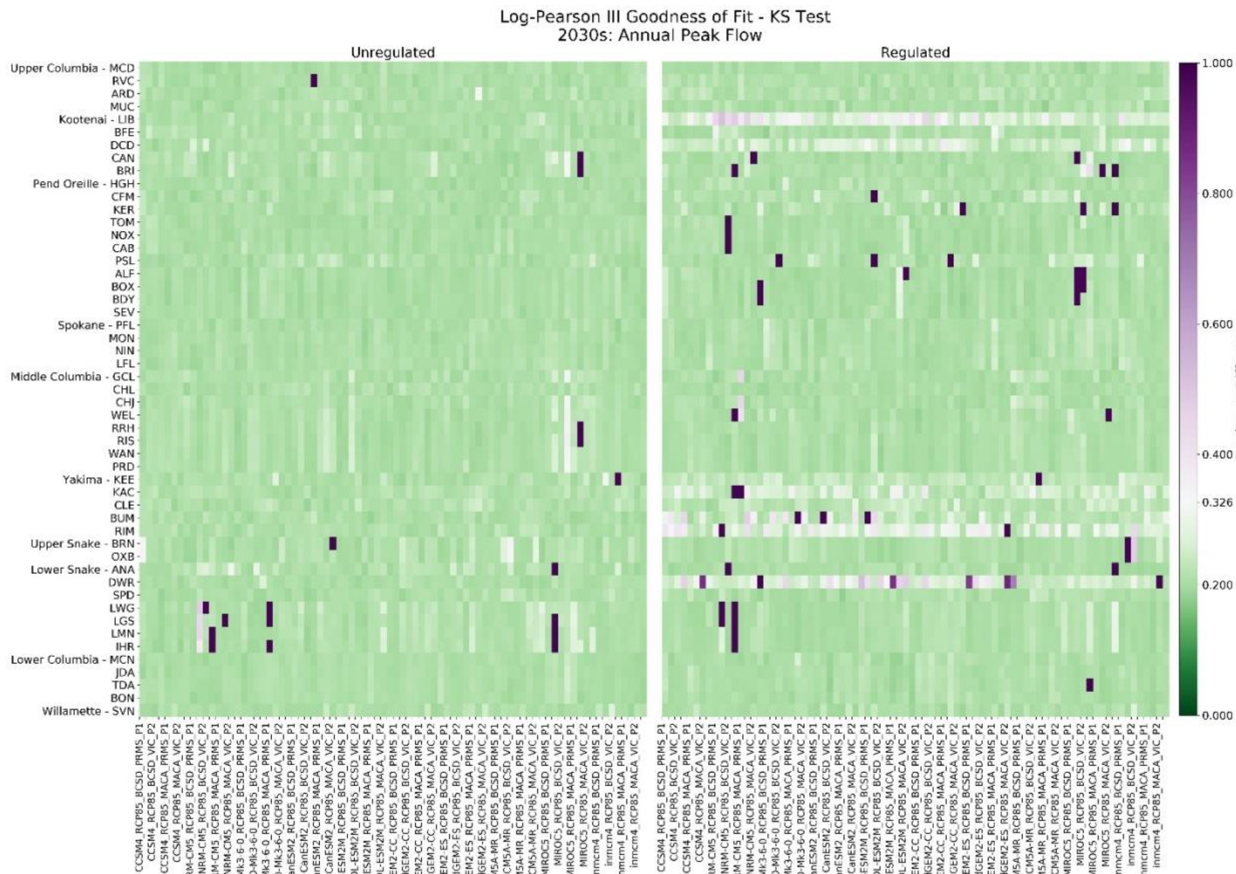


**Figure S4.** KS LP3 goodness of fit test results for 2030s annual peak flows for each ensemble member and each site included in the daily analysis. Test results are shown for unregulated analytical estimates (left) and regulated analytical estimates (right) and all 80 ensemble members (x-axis); however, only every other ensemble member is labelled. We accept the null hypothesis that the empirical and analytical populations are drawn from the same distributions if the maximum difference is less than the KS test statistic 0.326.

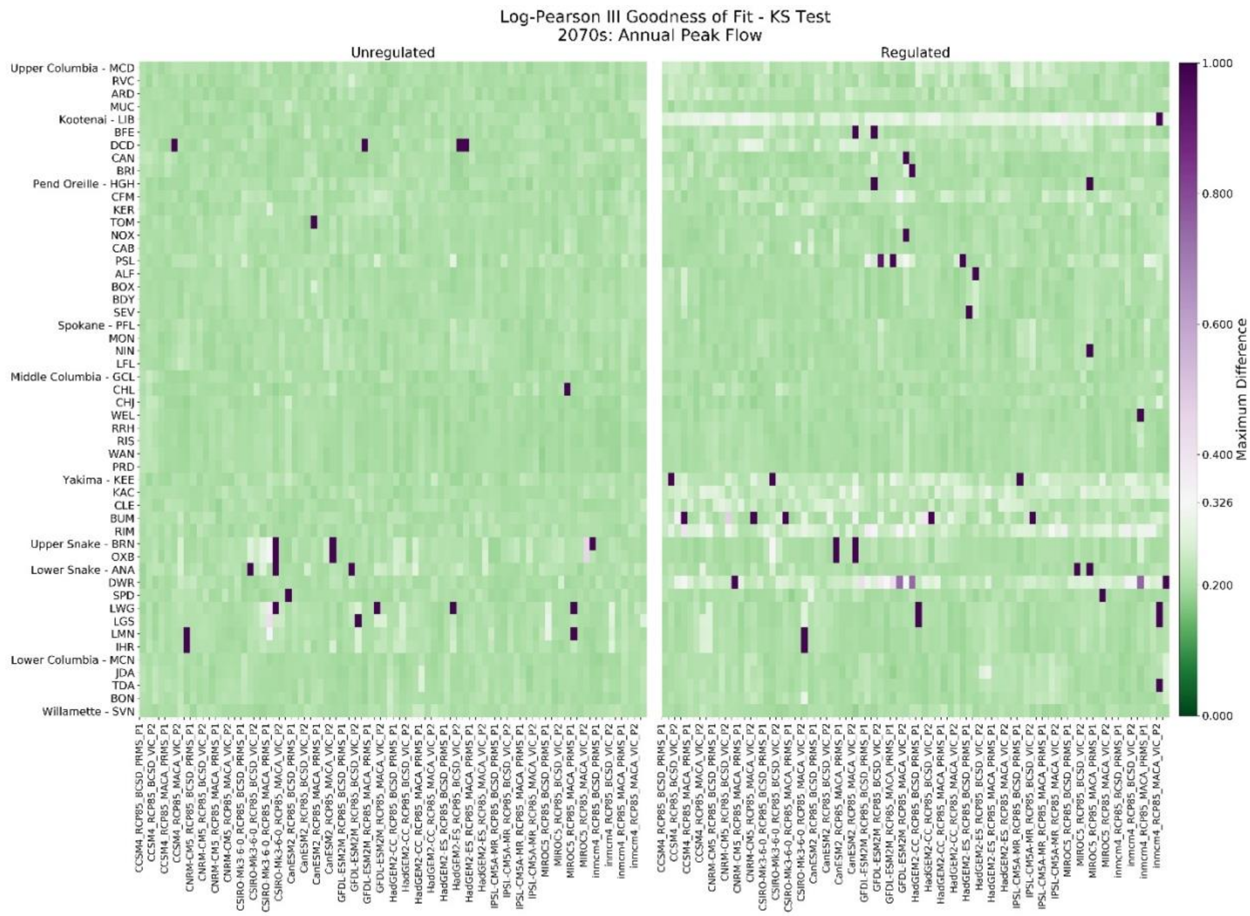


**Figure S5.** KS LP3 goodness of fit test results for 2070s annual peak flows for each ensemble member and each site included in the daily analysis. Test results are shown for unregulated analytical estimates (left) and regulated analytical estimates (right) and all 80 ensemble members (x-axis); however, only every other ensemble member is labelled. We accept the null hypothesis that the empirical and analytical populations are drawn from the same distributions if the maximum difference is less than the KS test statistic 0.326.

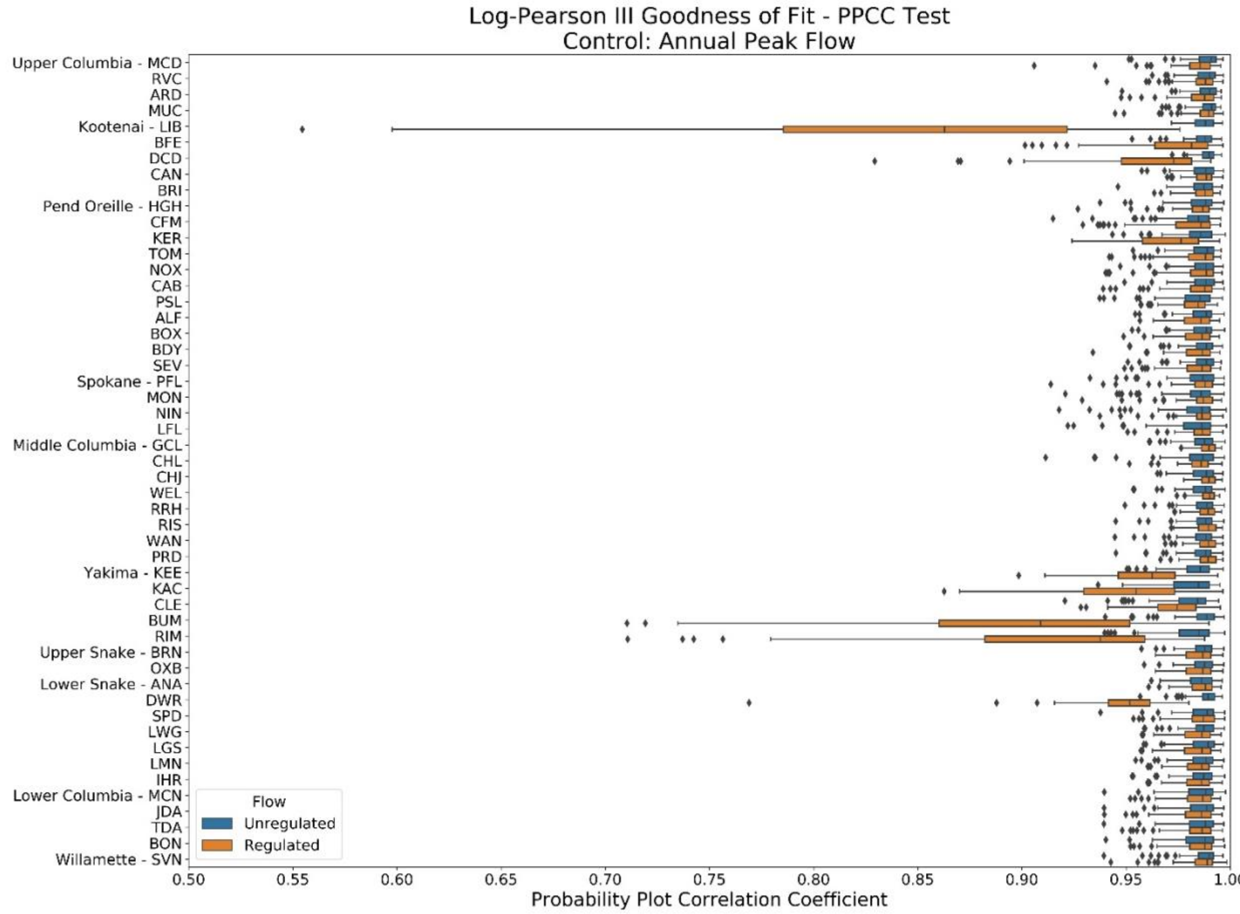


**Figure S6.** PPCC LP3 goodness of fit test results for control period annual peak flows for each site included in the daily analysis. Boxplots represent the distribution of test results for the 80-member ensemble for unregulated analytical estimates (orange) and regulated analytical estimates (blue). The analytical curve is a strong predictor of the empirical data if the probability plot correlation coefficient is near 1.

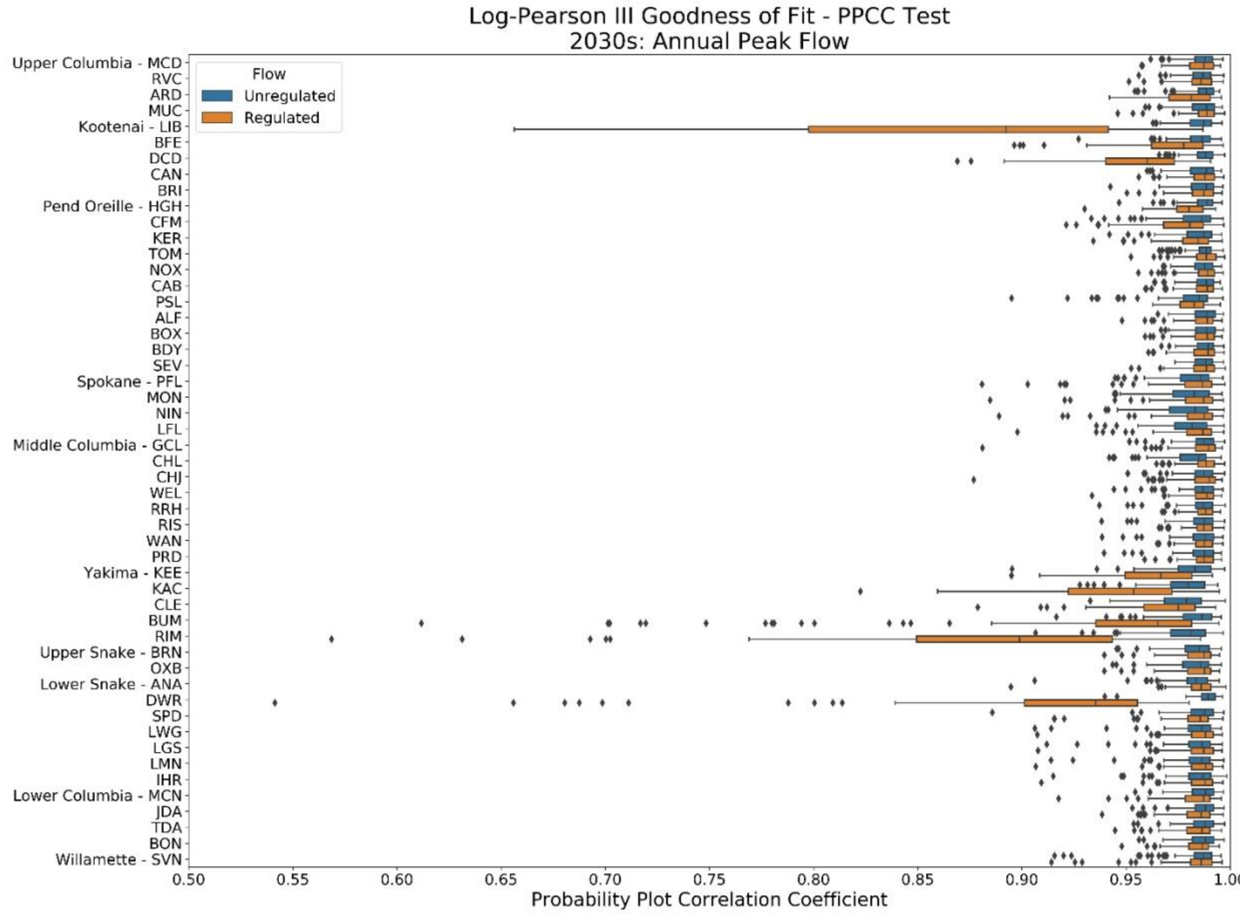


**Figure S7.** PPCC LP3 goodness of fit test results for 2030s annual peak flows for each site included in the daily analysis. Boxplots represent the distribution of test results for the 80-member ensemble for unregulated analytical estimates (orange) and regulated analytical estimates (blue). The analytical curve is a strong predictor of the empirical data if the probability plot correlation coefficient is near 1.

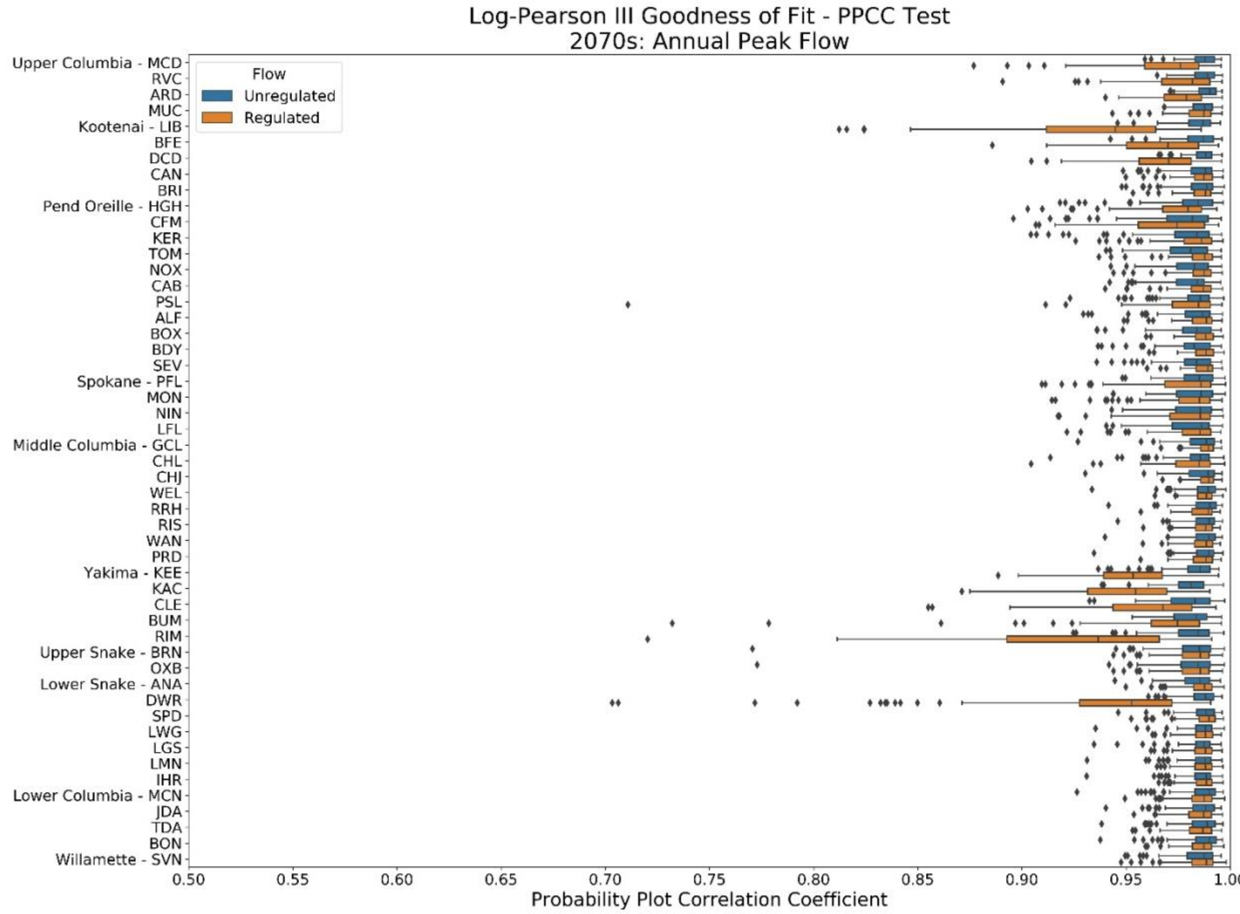


**Figure S8.** PPCC LP3 goodness of fit test results for 2070s annual peak flows for each site included in the daily analysis. Boxplots represent the distribution of test results for the 80-member ensemble for unregulated analytical estimates (orange) and regulated analytical estimates (blue). The analytical curve is a strong predictor of the empirical data if the probability plot correlation coefficient is near 1.

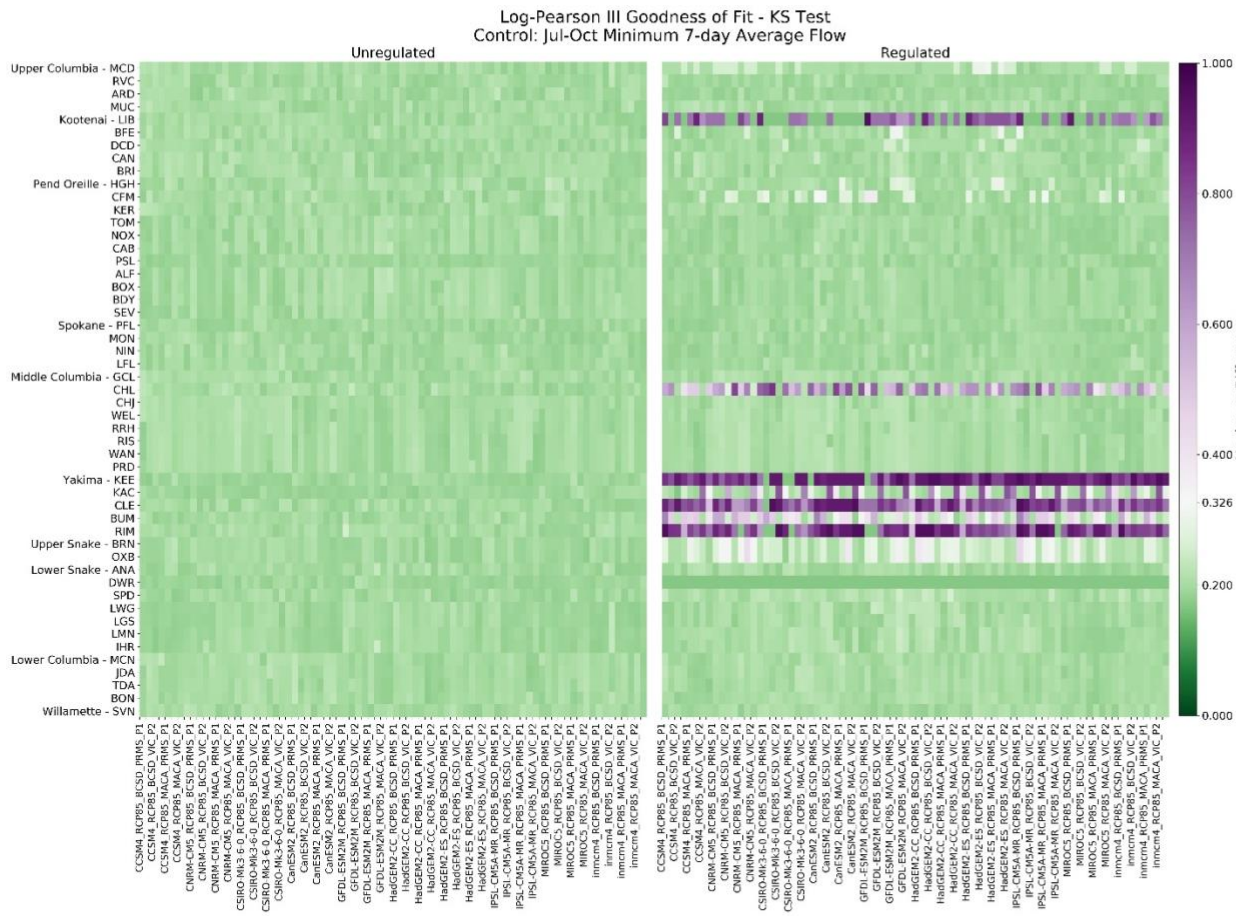


**Figure S9.** KS LP3 goodness of fit test results for control period annual minimum July-October 7-day average flows for each ensemble member and each site included in the daily analysis. Test results are shown for unregulated analytical estimates (left) and regulated analytical estimates (right) and all 80 ensemble members (x-axis); however, only every other ensemble member is labelled. We accept the null hypothesis that the empirical and analytical populations are drawn from the same distributions if the maximum difference is less than the KS test statistic 0.326.

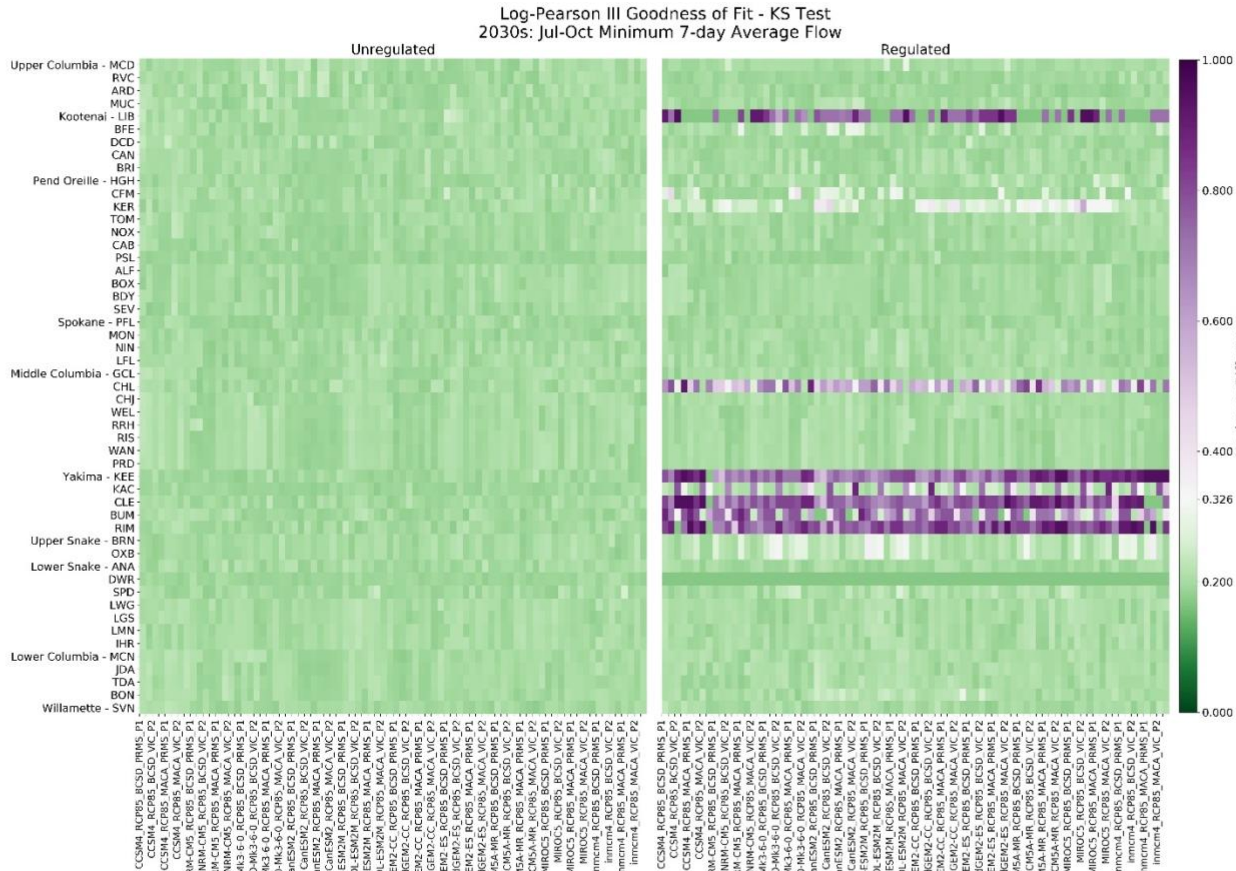


**Figure S10.** KS LP3 goodness of fit test results for 2030s annual minimum July-October 7-day average flows for each ensemble member and each site included in the daily analysis. Test results are shown for unregulated analytical estimates (left) and regulated analytical estimates (right) and all 80 ensemble members (x-axis); however, only every other ensemble member is labelled. We accept the null hypothesis that the empirical and analytical populations are drawn from the same distributions if the maximum difference is less than the KS test statistic 0.326.

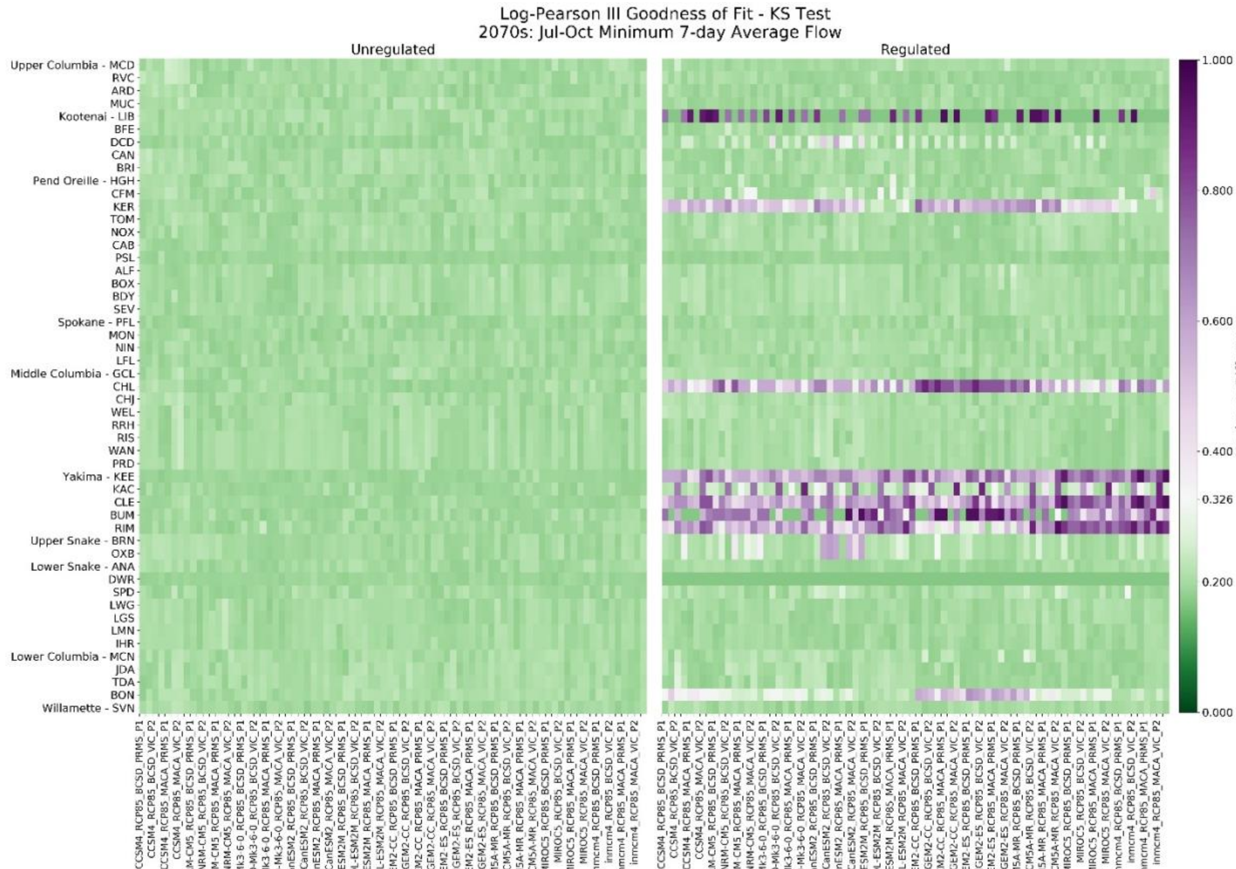


**Figure S11.** KS LP3 goodness of fit test results for 2070s annual minimum July-October 7-day average flows for each ensemble member and each site included in the daily analysis. Test results are shown for unregulated analytical estimates (left) and regulated analytical estimates (right) and all 80 ensemble members (x-axis); however, only every other ensemble member is labelled. We accept the null hypothesis that the empirical and analytical populations are drawn from the same distributions if the maximum difference is less than the KS test statistic 0.326.

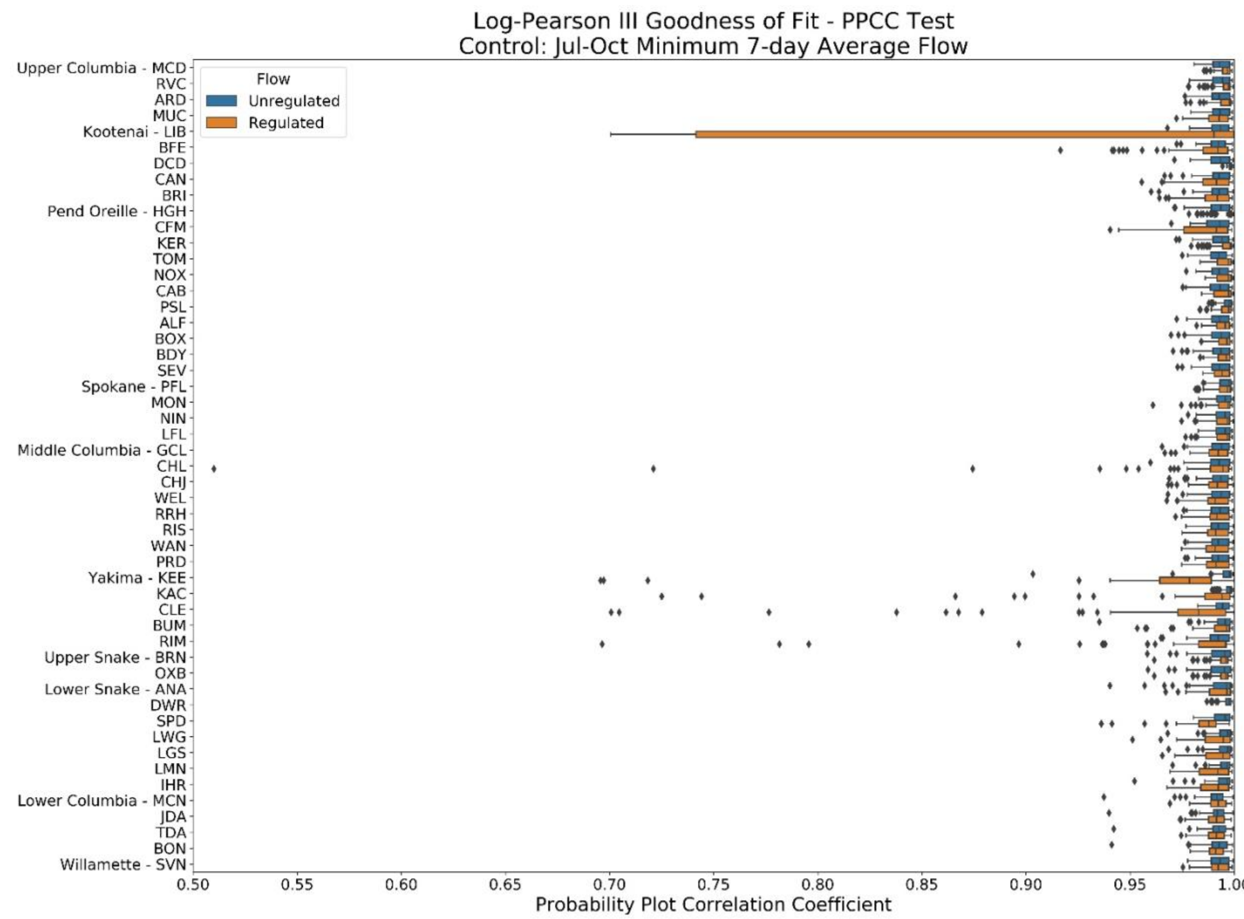


**Figure S12.** PPCC LP3 goodness of fit test results for control period annual minimum July-October 7-day average flows for each site included in the daily analysis. Boxplots represent the distribution of test results for the 80-member ensemble for unregulated analytical estimates (orange) and regulated analytical estimates (blue). The analytical curve is a strong predictor of the empirical data if the probability plot correlation coefficient is near 1.

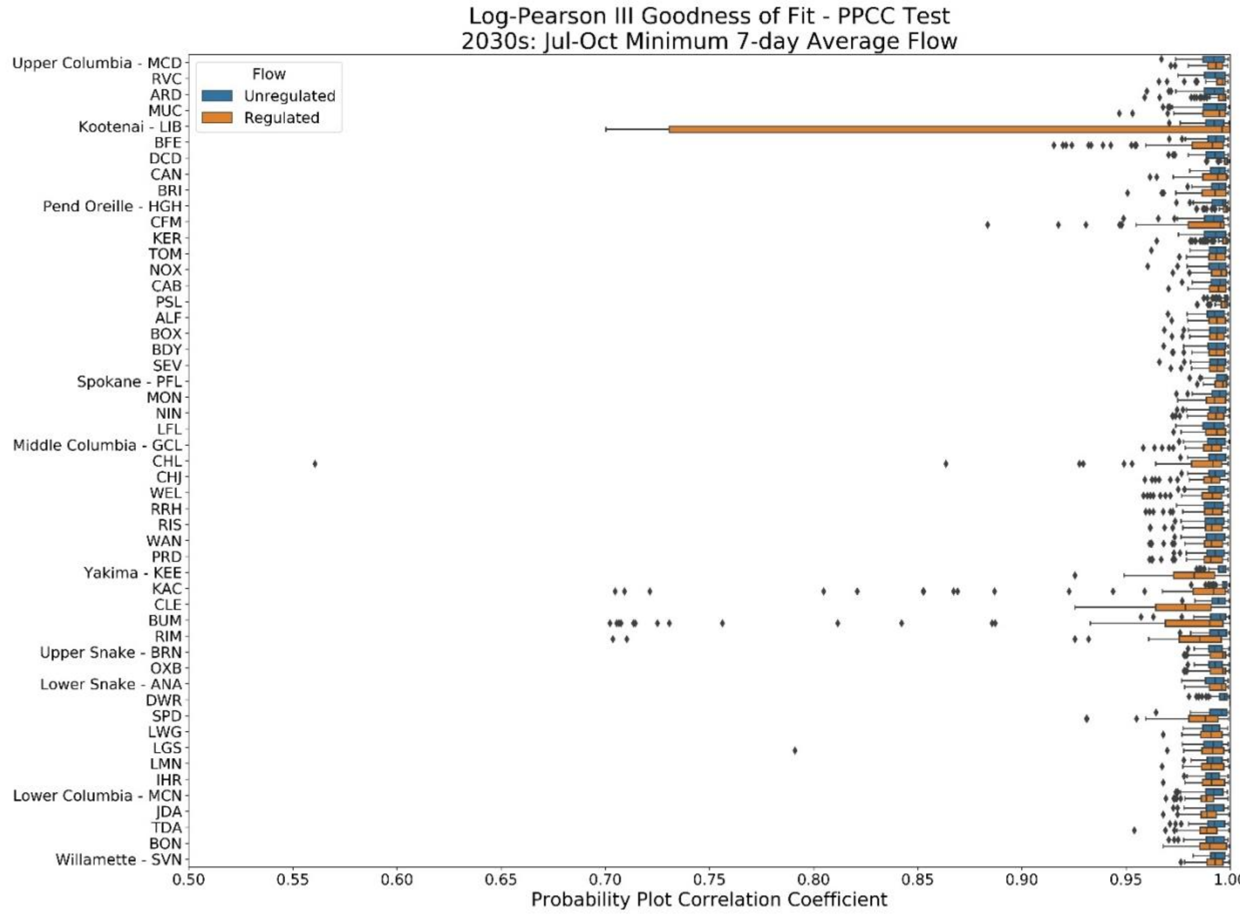


**Figure S13.** PPCC LP3 goodness of fit test results for 2030s annual minimum July-October 7-day average flows for each site included in the daily analysis. Boxplots represent the distribution of test results for the 80-member ensemble for unregulated analytical estimates (orange) and regulated analytical estimates (blue). The analytical curve is a strong predictor of the empirical data if the probability plot correlation coefficient is near 1.

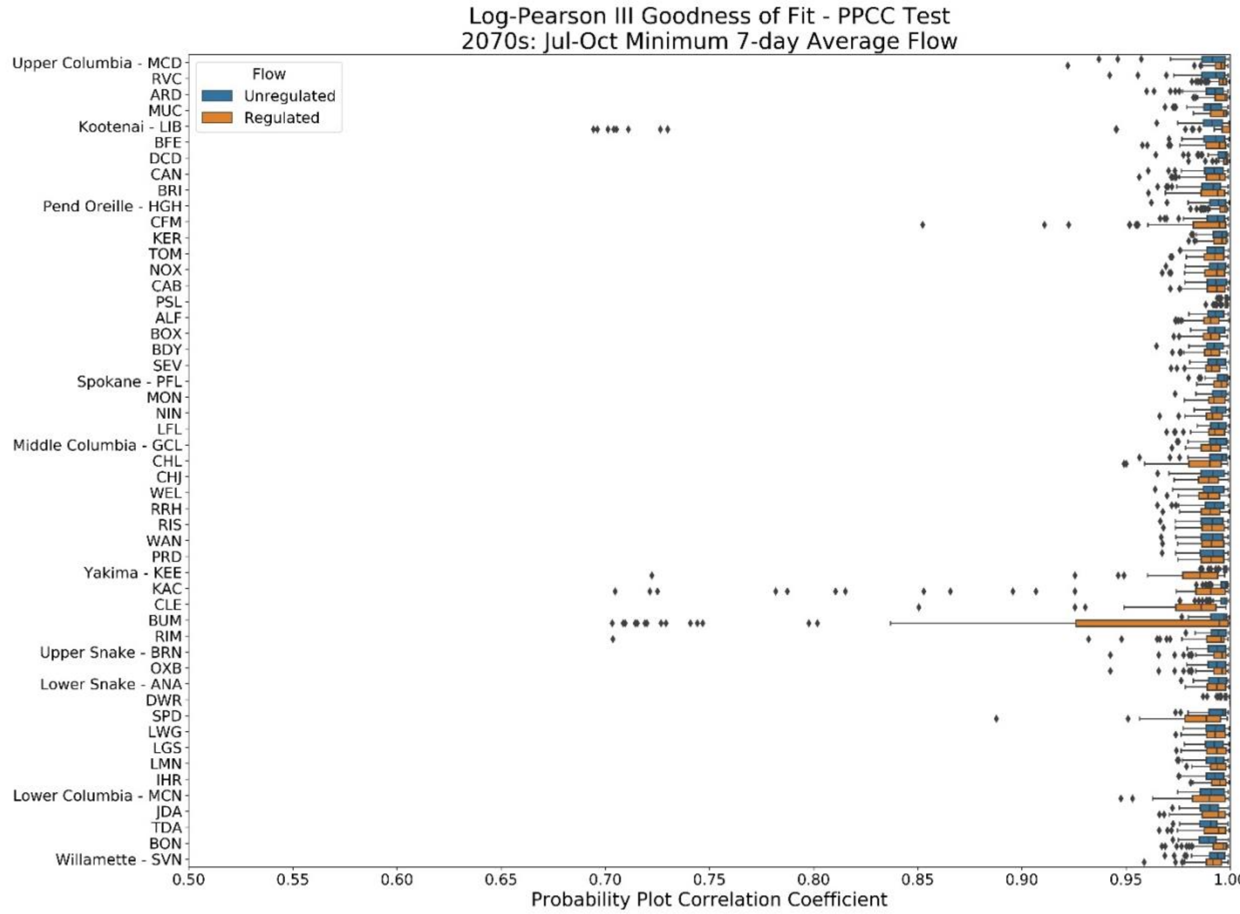


**Figure S14.** PPCC LP3 goodness of fit test results for 2070s annual minimum July-October 7-day average flows for each site included in the daily analysis. Boxplots represent the distribution of test results for the 80-member ensemble for unregulated analytical estimates (orange) and regulated analytical estimates (blue). The analytical curve is a strong predictor of the empirical data if the probability plot correlation coefficient is near 1.

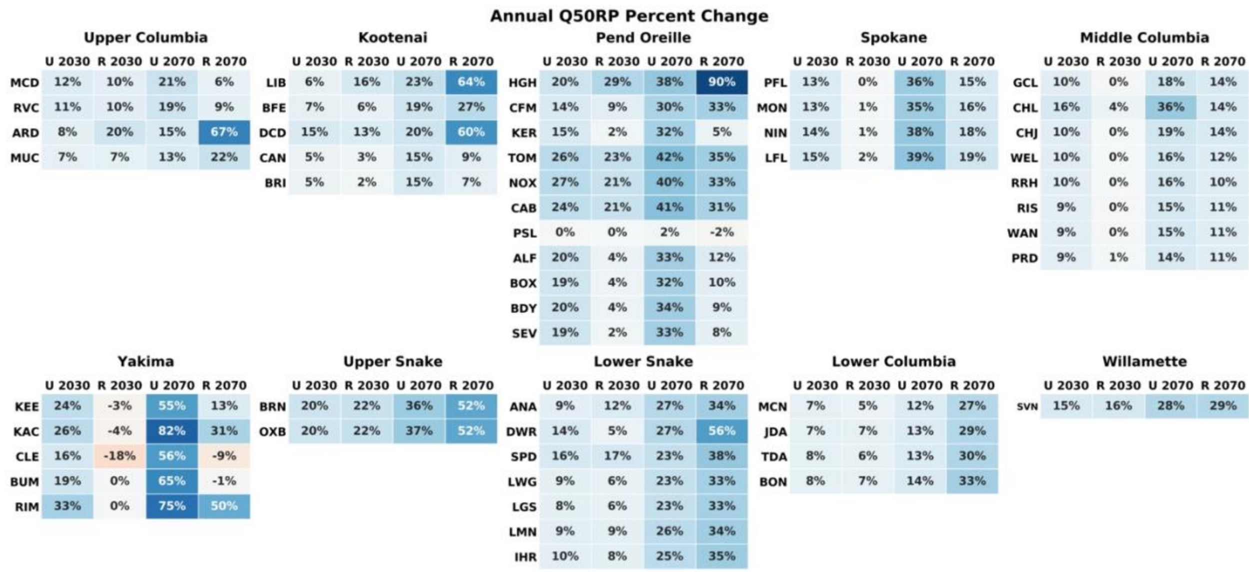


**Figure S15.** Median percent change of annual Q50RP flow for unregulated conditions (U) and regulated conditions (R). For each region, locations are sorted from upstream (top) to downstream (bottom) based on position of confluence with the next lowest order stream using a top-down stream order approach (e.g., a headwater tributary has a higher stream order than the mainstem).

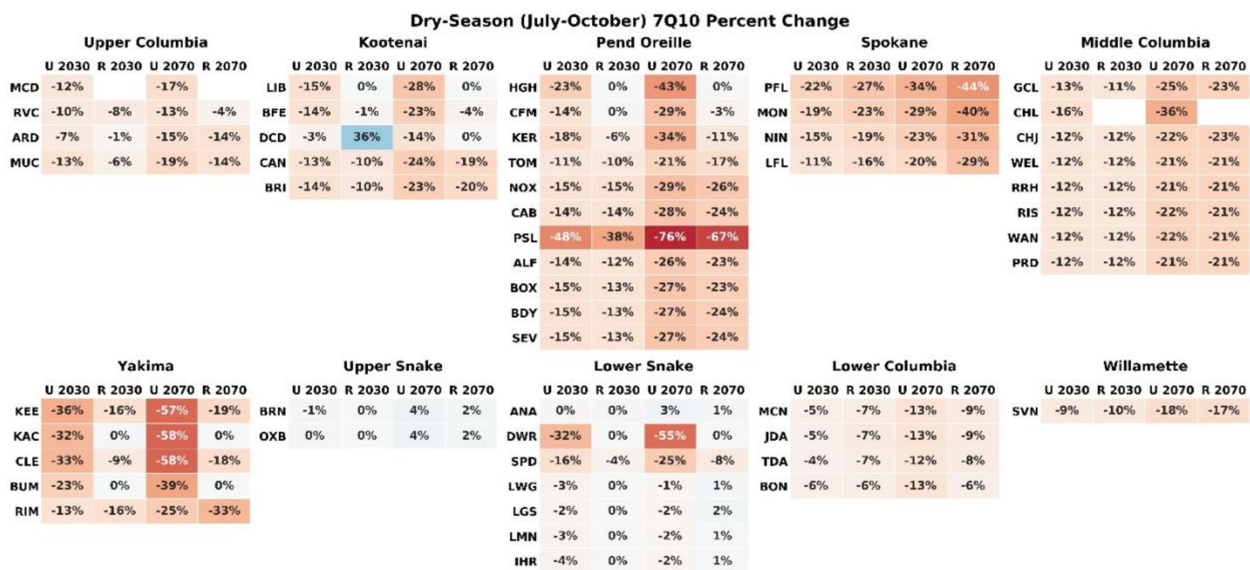


**Figure S16.** Median percent change of annual 7Q10 flow for unregulated conditions (U) and regulated conditions (R). For each region, locations are sorted from upstream (top) to downstream (bottom) based on position of confluence with the next lowest order stream using a top-down stream order approach (e.g., a headwater tributary has a higher stream order than the mainstem). Locations where the heatmap is blank exhibited infinite or invalid values as a result of near-zero or zero 7Q10 flows in the numerator or the denominator.

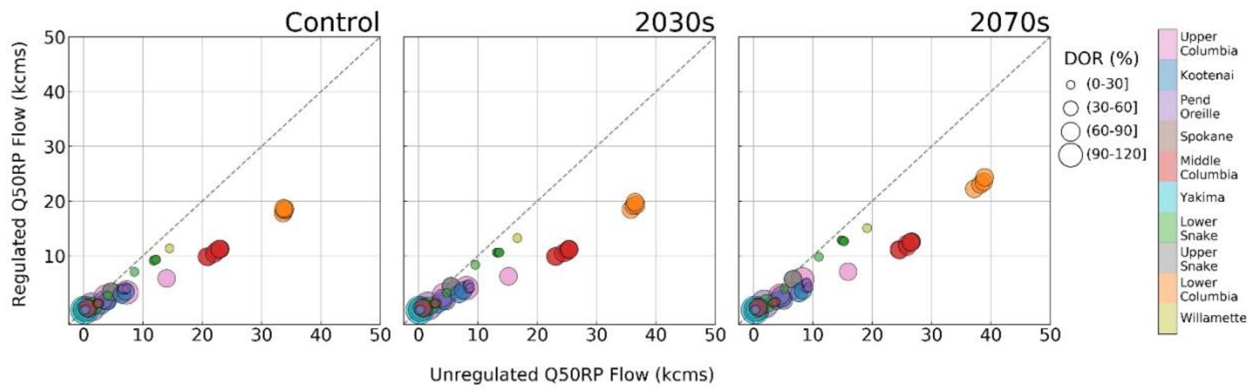


**Figure S17.** Annual 50-year return period peak flows (Q50RP) for unregulated conditions (x-axis) and regulated conditions (y-axis). Figure shows the median Q50RP flows across the 80-member ensemble. Points are colored by region and sized by the degree of upstream regulation (DOR). In the absence of regulation, points would fall on the dashed 1:1 line.

**Table S1.** Details about the 75 locations cited in the main text including drainage area and control period (1976-2005) regime. For each region, locations are sorted from upstream (top) to downstream (bottom) based on position of tributary confluence with the next lowest order stream using a top-down stream order approach (e.g., a headwater tributary has a higher stream order than the mainstem).

| Region | Site ID | Location | River | Drainage Area (km$^2$) | Control Regime |
|---|---|---|---|---|---|
| Upper Columbia | MCD | Mica | Columbia River | 21471 | snow |
| | RVC | Revelstoke | Columbia River | 26418 | snow |
| | ARD | Arrow Lakes | Columbia River | 36519 | snow |
| | MUC | Birchbank | Columbia River | 88099 | snow |
| Kootenai | LIB | Libby | Kootenai River | 23271 | snow |
| | BFE | Bonners Ferry | Kootenai River | 32867 | snow |
| | DCD | Duncan | Duncan River | 1331 | snow |
| | CAN | Corra Linn | Kootenai River | 45584 | snow |
| | BRI | Brilliant | Kootenai River | 49987 | snow |
| Pend Oreille | HGH | Hungry Horse | South Fork Flathead River | 4284 | snow |
| | CFM | Columbia Falls | Flathead River | 11562 | snow |
| | KER | Kerr | Flathead River | 18353 | snow |
| | TOM | Thompson Falls | Clark Fork | 54682 | snow |
| | NOX | Noxon Rapids | Clark Fork | 56547 | snow |
| | CAB | Cabinet Gorge | Clark Fork | 57169 | snow |
| | PSL | Priest Lake | Priest River | 1481 | snow |
| | ALF | Albeni Falls | Pend Oreille River | 62678 | snow |
| | BOX | Box Canyon | Pend Oreille River | 64491 | snow |
| | BDY | Boundary | Pend Oreille River | 65268 | snow |
| | SEV | Waneta | Pend Oreille River | 66822 | snow |
| Spokane | PFL | Post Falls | Spokane River | 9946 | snow |

| | | | | | |
|---|---|---|---|---|---|
| | MON | Monroe Street | Spokane River | 11111 | snow |
| | NIN | Nine Mile | Spokane River | 13468 | transient |
| | LFL | Long Lake | Spokane River | 15592 | transient |
| Middle Columbia | GCL | Grand Coulee | Columbia River | 193472 | snow |
| | CHL | Chelan | Chelan River | 2393 | snow |
| | CHJ | Chief Joseph | Columbia River | 195285 | snow |
| | WEL | Wells | Columbia River | 222998 | snow |
| | RRH | Rocky Reach | Columbia River | 227401 | snow |
| | RIS | Rock Island | Columbia River | 231545 | snow |
| | WAN | Wanapum | Columbia River | 234912 | snow |
| | PRD | Priest Rapids | Columbia River | 248639 | snow |
| Yakima | KEE | Keechelus | Yakima River | 142 | transient |
| | KAC | Kachess | Kachess River | 166 | transient |
| | CLE | Cle Elum | Cle Elum River | 526 | snow |
| | BUM | Bumping Lake | Bumping River | 184 | snow |
| | RIM | Rimrock - Tieton | Tieton River | 484 | snow |
| Upper Snake | JCKY | Jackson Lake | Snake River | 2090 | snow |
| | PALI | Snake nr Irwin Palisades | Snake River | 13533 | snow |
| | HEII | Snake nr Heise | Snake River | 14898 | snow |
| | LORI | Lorenzo | Snake River | 15048 | snow |
| | REXI | Henry's Fork nr Rexburg | Henrys Fork | 7563 | rain |
| | SHYI | Snake nr Shelley | Snake River | 25356 | snow |
| | BFTI | Snake nr Blackfoot | Snake River | 29293 | snow |
| | AMFI | American Falls | Snake River | 35224 | snow |
| | MILI | Milner | Snake River | 44496 | snow |
| | KIMI | Snake nr Kimberly | Snake River | 57860 | snow |
| | SKHI | King Hill | Snake River | 92722 | snow |
| | SWAI | Snake nr Murphy | Snake River | 108521 | transient |
| | ANDI | Anderson Ranch | South Fork Boise River | 2533 | snow |
| | ARKI | Arrowrock | Boise River | 5739 | snow |
| | LUCI | Lucky Peak | Boise River | 6941 | snow |
| | BIGI | Glenwood Bridge | Boise River | 7182 | snow |
| | OWY | Owyhee River nr Rome OR | Owyhee River | 28904 | rain |
| | SNYI | Nyssa | Snake River | 152032 | transient |
| | DEDI | Deadwood | Deadwood River | 290 | snow |
| | PABI | Payette NF+SF | Payette River | 1181 | snow |
| | HRSI | Horseshoe Bend | Payette River | 5750 | snow |
| | PRPI | Payette | Payette River | 8392 | snow |
| | WEII | Weiser | Weiser River | 3755 | transient |
| | BRN | Brownlee | Snake River | 188007 | transient |

| | | | | | |
|---|---|---|---|---|---|
| | OXB | Oxbow | Snake River | 188551 | transient |
| Lower Snake | ANA | Anatone | Snake River | 240765 | snow |
| | DWR | Dworshak | North Fork Clearwater River | 6320 | snow |
| | SPD | Spalding | Clearwater River | 24786 | snow |
| | LWG | Lower Granite | Snake River | 267287 | snow |
| | LGS | Little Goose | Snake River | 269100 | snow |
| | LMN | Lower Monumental | Snake River | 281014 | snow |
| | IHR | Ice Harbor | Snake River | 281014 | snow |
| | MCN | McNary | Columbia River | 554258 | snow |
| Lower Columbia | JDA | John Day | Columbia River | 585338 | snow |
| | TDA | The Dalles | Columbia River | 613828 | snow |
| | BON | Bonneville | Columbia River | 621339 | snow |
| Willamette | SVN | T.W. Sullivan | Willamette River | 25900 | transient |

**Table S2.** September-November (SON) Volume Percent Change. U is unregulated, R is regulated. Table shows the (10th) 50th (90th) percentiles of the ensemble. For each region, locations are sorted from upstream (top) to downstream (bottom) based on position of tributary confluence with the next lowest order stream using a top-down stream order approach (e.g., a headwater tributary has a higher stream order than the mainstem).

**SON**

| Region | Site ID | 2030 U | 2030 R | 2070 U | 2070 R |
|---|---|---|---|---|---|
| Upper Columbia | MCD | (-18) -11 (0) | (-5) 5 (15) | (-29) -14 (13) | (3) 20 (30) |
| | RVC | (-16) -9 (1) | (-6) 4 (12) | (-22) -8 (18) | (4) 17 (29) |
| | ARD | (-16) -7 (4) | (-11) -6 (-2) | (-20) -5 (20) | (-22) -11 (-4) |
| | MUC | (-17) -8 (5) | (-13) -8 (-2) | (-20) -8 (17) | (-23) -12 (-4) |
| Kootenai | LIB | (-21) -10 (6) | (-19) -11 (-2) | (-28) -12 (11) | (-31) -18 (-4) |
| | BFE | (-19) -8 (8) | (-16) -10 (0) | (-25) -12 (14) | (-30) -15 (0) |
| | DCD | (-19) -7 (13) | (-16) -9 (0) | (-32) 2 (34) | (-24) -13 (8) |
| | CAN | (-17) -8 (7) | (-17) -12 (0) | (-25) -12 (17) | (-28) -14 (2) |
| | BRI | (-18) -8 (8) | (-17) -11 (0) | (-24) -11 (17) | (-27) -15 (3) |
| Pend Oreille | HGH | (-27) -8 (14) | (-7) -1 (5) | (-39) -19 (20) | (-10) -1 (5) |
| | CFM | (-25) -5 (17) | (-10) -3 (8) | (-30) -13 (24) | (-14) -5 (13) |
| | KER | (-23) -6 (11) | (-14) -8 (0) | (-32) -15 (20) | (-36) -17 (-6) |
| | TOM | (-16) -3 (10) | (-13) -5 (2) | (-25) -9 (19) | (-29) -12 (1) |
| | NOX | (-17) -5 (9) | (-13) -6 (1) | (-26) -11 (16) | (-30) -13 (0) |
| | CAB | (-17) -4 (9) | (-14) -6 (2) | (-26) -10 (16) | (-30) -12 (0) |
| | PSL | (-17) -2 (20) | (-10) -4 (6) | (-15) 10 (43) | (-12) -1 (12) |
| | ALF | (-15) -3 (10) | (-9) -4 (1) | (-23) -8 (17) | (-20) -9 (0) |
| | BOX | (-15) -3 (10) | (-9) -4 (1) | (-23) -8 (17) | (-21) -9 (0) |

| | | | | | |
|---|---|---|---|---|---|
| | BDY | (-15) -3 (10) | (-9) -4 (1) | (-23) -8 (16) | (-21) -9 (0) |
| | SEV | (-15) -3 (10) | (-10) -4 (1) | (-23) -7 (16) | (-21) -9 (0) |
| Spokane | PFL | (-20) -2 (31) | (-13) -3 (12) | (-19) 2 (55) | (-15) -4 (19) |
| | MON | (-19) -3 (24) | (-13) -4 (11) | (-18) -1 (42) | (-15) -5 (15) |
| | NIN | (-18) -2 (24) | (-13) -3 (10) | (-17) 0 (35) | (-14) -4 (14) |
| | LFL | (-17) -2 (22) | (-13) -3 (10) | (-15) 1 (29) | (-14) -3 (12) |
| Middle Columbia | GCL | (-15) -5 (8) | (-11) -7 (0) | (-19) -6 (19) | (-21) -12 (-2) |
| | CHL | (-16) -3 (14) | (-12) -4 (8) | (-19) 5 (44) | (-21) -6 (20) |
| | CHJ | (-15) -5 (8) | (-11) -7 (0) | (-19) -7 (19) | (-21) -12 (-2) |
| | WEL | (-15) -4 (9) | (-11) -7 (0) | (-18) -5 (19) | (-20) -11 (-1) |
| | RRH | (-15) -5 (9) | (-11) -7 (0) | (-18) -5 (19) | (-20) -11 (0) |
| | RIS | (-15) -4 (9) | (-11) -6 (0) | (-17) -4 (19) | (-19) -10 (0) |
| | WAN | (-15) -4 (9) | (-11) -7 (0) | (-17) -4 (19) | (-20) -10 (0) |
| | PRD | (-15) -5 (9) | (-11) -7 (0) | (-17) -4 (19) | (-20) -10 (0) |
| Yakima | KEE | (-29) 0 (19) | (-31) -20 (-6) | (-39) 10 (34) | (-42) -30 (-20) |
| | KAC | (-26) 0 (25) | (-8) 0 (6) | (-39) 13 (39) | (-30) -12 (4) |
| | CLE | (-23) -2 (18) | (-39) -27 (-17) | (-34) 8 (35) | (-49) -38 (-25) |
| | BUM | (-18) -2 (21) | (-19) -6 (11) | (-20) 2 (49) | (-25) -4 (22) |
| | RIM | (-18) -3 (14) | (-5) -1 (5) | (-24) -4 (29) | (-21) -9 (1) |
| Upper Snake | JCKY | (-8) 0 (9) | (-5) 0 (3) | (-13) 1 (30) | (-19) -8 (2) |
| | PALI | (-5) 0 (13) | (-13) -7 (4) | (-7) 6 (28) | (-26) -12 (8) |
| | HEII | (-5) 0 (12) | (-12) -6 (5) | (-7) 6 (26) | (-24) -10 (9) |
| | LORI | (-5) 0 (12) | (-13) -5 (12) | (-7) 6 (26) | (-24) -7 (21) |
| | REXI | (-5) 0 (12) | (-3) 2 (10) | (-13) 0 (20) | (-6) 3 (16) |
| | SHYI | (-7) -1 (10) | (-11) -3 (10) | (-15) 0 (18) | (-23) -9 (13) |
| | BFTI | (-7) -1 (11) | (-12) -2 (13) | (-15) 0 (19) | (-26) -9 (17) |
| | AMFI | (-6) 0 (11) | (-15) -8 (1) | (-11) 2 (26) | (-31) -19 (-3) |
| | MILI | (-5) 0 (10) | (-36) -14 (14) | (-11) 2 (30) | (-56) -35 (14) |
| | KIMI | (-5) 0 (11) | (-27) -10 (13) | (-10) 3 (31) | (-42) -24 (15) |
| | SKHI | (-2) 3 (13) | (-4) 3 (11) | (-1) 8 (42) | (-1) 5 (30) |
| | SWAI | (-1) 5 (16) | (-2) 6 (14) | (0) 10 (44) | (0) 10 (37) |
| | ANDI | (-2) 11 (31) | (-9) 1 (9) | (5) 25 (60) | (-18) 0 (14) |
| | ARKI | (-2) 10 (29) | (-13) 2 (23) | (2) 20 (52) | (-19) 4 (33) |
| | LUCI | (-2) 9 (28) | (-14) -1 (9) | (1) 18 (52) | (-22) -3 (13) |
| | BIGI | (-2) 7 (24) | (-18) -1 (27) | (-2) 14 (46) | (-12) 12 (62) |
| | OWY | (0) 27 (65) | (-6) 2 (14) | (-2) 48 (143) | (-8) 5 (94) |
| | SNYI | (-1) 8 (20) | (-4) 4 (15) | (1) 14 (47) | (-1) 11 (39) |
| | DEDI | (-16) -4 (30) | (-15) 6 (30) | (-30) 1 (59) | (-14) 13 (38) |
| | PABI | (-13) 1 (26) | (-14) -4 (7) | (-27) 9 (54) | (-24) -13 (3) |
| | HRSI | (-10) 4 (27) | (-7) 1 (19) | (-17) 10 (47) | (-12) 4 (29) |

| | | | | | |
|---|---|---|---|---|---|
| | PRPI | (-16) 1 (23) | (-26) -12 (13) | (-29) 6 (43) | (-38) -15 (24) |
| | WEII | (-2) 8 (22) | (-5) 3 (14) | (1) 15 (44) | (-3) 9 (35) |
| | BRN | (-2) 7 (23) | (-5) 3 (14) | (1) 15 (43) | (-2) 9 (35) |
| | OXB | (-2) 7 (22) | (-5) 3 (14) | (1) 15 (43) | (-2) 9 (35) |
| Lower Snake | ANA | (-5) 4 (17) | (-6) 2 (15) | (-2) 9 (37) | (-4) 6 (31) |
| | DWR | (-15) -5 (17) | (-16) -8 (-2) | (-20) -4 (27) | (-26) -12 (-1) |
| | SPD | (-17) -4 (20) | (-16) -7 (6) | (-22) -4 (30) | (-21) -10 (11) |
| | LWG | (-7) 3 (16) | (-7) 0 (12) | (-5) 6 (34) | (-7) 2 (25) |
| | LGS | (-7) 3 (16) | (-7) 0 (12) | (-5) 6 (33) | (-7) 2 (25) |
| | LMN | (-8) 2 (16) | (-8) 0 (12) | (-6) 5 (32) | (-9) 0 (22) |
| | IHR | (-8) 2 (16) | (-8) 0 (12) | (-6) 5 (31) | (-9) 0 (22) |
| | MCN | (-10) -2 (9) | (-10) -5 (2) | (-14) 0 (20) | (-17) -9 (4) |
| Lower Columbia | JDA | (-11) -2 (9) | (-10) -5 (1) | (-14) 0 (20) | (-17) -9 (4) |
| | TDA | (-10) -2 (9) | (-10) -5 (2) | (-13) 0 (20) | (-17) -9 (4) |
| | BON | (-10) -2 (8) | (-10) -5 (1) | (-13) -1 (19) | (-17) -9 (3) |
| Willamette | SVN | (-15) -2 (10) | (-16) -3 (8) | (-27) -4 (10) | (-27) -6 (8) |

**Table S3.** December-February (DJF) Volume Percent Change. U is unregulated, R is regulated. Table shows the (10th) 50th (90th) percentiles of the ensemble. For each region, locations are sorted from upstream (top) to downstream (bottom) based on position of tributary confluence with the next lowest order stream using a top-down stream order approach (e.g., a headwater tributary has a higher stream order than the mainstem).

**DJF**

| Region | Site ID | 2030 U | 2030 R | 2070 U | 2070 R |
|---|---|---|---|---|---|
| Upper Columbia | MCD | (-3) 17 (41) | (-12) -8 (0) | (10) 56 (106) | (-33) -18 (-7) |
| | RVC | (-2) 21 (44) | (-10) -6 (2) | (12) 65 (116) | (-27) -12 (0) |
| | ARD | (0) 24 (49) | (-8) -1 (2) | (16) 73 (120) | (-25) -5 (4) |
| | MUC | (3) 22 (48) | (-8) 0 (7) | (35) 66 (120) | (-13) 0 (13) |
| Kootenai | LIB | (-4) 14 (36) | (-17) -2 (10) | (14) 56 (105) | (-21) -2 (14) |
| | BFE | (0) 22 (51) | (-14) 2 (13) | (39) 66 (134) | (-9) 10 (32) |
| | DCD | (-2) 24 (51) | (-7) 1 (9) | (10) 80 (127) | (-22) 0 (15) |
| | CAN | (1) 23 (51) | (-10) 5 (15) | (44) 66 (134) | (0) 8 (38) |
| | BRI | (1) 22 (50) | (-10) 5 (16) | (43) 65 (133) | (2) 10 (40) |
| Pend Oreille | HGH | (-1) 40 (86) | (-24) -12 (6) | (44) 140 (266) | (-40) -23 (9) |
| | CFM | (4) 40 (82) | (-8) 5 (23) | (48) 137 (246) | (1) 26 (76) |
| | KER | (5) 40 (80) | (-4) 4 (16) | (51) 133 (235) | (0) 16 (49) |
| | TOM | (4) 34 (68) | (-2) 11 (25) | (59) 100 (184) | (16) 29 (74) |
| | NOX | (5) 38 (77) | (-1) 12 (29) | (68) 114 (211) | (19) 32 (80) |
| | CAB | (4) 36 (75) | (-1) 14 (31) | (66) 108 (202) | (21) 34 (84) |

| | | | | | |
|---|---|---|---|---|---|
| | PSL | (9) 58 (101) | (4) 50 (91) | (78) 178 (281) | (53) 137 (230) |
| | ALF | (6) 36 (71) | (0) 17 (35) | (63) 103 (194) | (24) 38 (82) |
| | BOX | (6) 35 (70) | (0) 17 (35) | (62) 102 (192) | (24) 39 (82) |
| | BDY | (6) 35 (70) | (0) 17 (35) | (61) 100 (191) | (24) 39 (83) |
| | SEV | (5) 34 (71) | (-1) 17 (36) | (60) 100 (192) | (25) 41 (85) |
| Spokane | PFL | (24) 69 (108) | (22) 61 (105) | (114) 178 (223) | (106) 167 (205) |
| | MON | (18) 60 (98) | (17) 53 (92) | (104) 158 (190) | (93) 147 (177) |
| | NIN | (15) 55 (92) | (15) 49 (87) | (97) 148 (172) | (86) 136 (162) |
| | LFL | (14) 51 (88) | (14) 45 (81) | (90) 139 (162) | (78) 122 (146) |
| Middle Columbia | GCL | (6) 30 (55) | (-6) 6 (15) | (55) 84 (143) | (3) 12 (32) |
| | CHL | (-5) 34 (75) | (-1) 3 (10) | (13) 130 (210) | (0) 15 (28) |
| | CHJ | (6) 30 (54) | (-6) 6 (15) | (54) 83 (142) | (3) 12 (32) |
| | WEL | (5) 30 (54) | (-6) 6 (15) | (54) 85 (143) | (3) 13 (34) |
| | RRH | (5) 30 (55) | (-6) 6 (15) | (54) 85 (145) | (3) 13 (34) |
| | RIS | (5) 30 (57) | (-5) 7 (16) | (55) 89 (148) | (4) 14 (36) |
| | WAN | (5) 30 (57) | (-5) 7 (16) | (55) 89 (149) | (4) 14 (37) |
| | PRD | (5) 30 (57) | (-5) 7 (16) | (55) 90 (149) | (4) 14 (37) |
| Yakima | KEE | (19) 52 (85) | (-18) 1 (31) | (90) 131 (174) | (-16) 21 (63) |
| | KAC | (16) 52 (84) | (-19) -3 (12) | (89) 135 (184) | (-18) 4 (74) |
| | CLE | (2) 51 (91) | (-30) -10 (17) | (60) 179 (289) | (-32) 6 (51) |
| | BUM | (15) 58 (107) | (8) 28 (70) | (95) 186 (273) | (52) 104 (184) |
| | RIM | (7) 34 (78) | (-27) -10 (72) | (64) 110 (185) | (-21) 29 (253) |
| Upper Snake | JCKY | (-3) 9 (29) | (-6) -1 (7) | (7) 57 (149) | (-6) 5 (33) |
| | PALI | (2) 16 (38) | (-9) 7 (27) | (24) 65 (142) | (7) 37 (94) |
| | HEII | (3) 16 (37) | (-7) 9 (28) | (25) 63 (133) | (10) 38 (92) |
| | LORI | (3) 16 (37) | (-7) 10 (28) | (26) 63 (133) | (10) 39 (94) |
| | REXI | (4) 22 (39) | (0) 13 (25) | (26) 72 (135) | (14) 42 (82) |
| | SHYI | (5) 22 (43) | (-4) 13 (30) | (32) 82 (172) | (15) 47 (106) |
| | BFTI | (5) 23 (44) | (-3) 13 (30) | (35) 88 (184) | (15) 47 (107) |
| | AMFI | (6) 23 (43) | (-18) 4 (36) | (36) 82 (164) | (-11) 35 (116) |
| | MILI | (8) 28 (46) | (-16) 6 (35) | (40) 85 (162) | (-4) 43 (118) |
| | KIMI | (8) 27 (45) | (-15) 7 (35) | (39) 82 (154) | (-2) 43 (113) |
| | SKHI | (6) 25 (38) | (-6) 11 (26) | (33) 70 (131) | (3) 37 (93) |
| | SWAI | (6) 24 (41) | (-4) 14 (31) | (31) 68 (122) | (6) 40 (95) |
| | ANDI | (10) 48 (105) | (-12) 10 (51) | (50) 178 (365) | (10) 63 (176) |
| | ARKI | (21) 57 (110) | (-12) 11 (53) | (84) 190 (331) | (19) 91 (226) |
| | LUCI | (21) 60 (112) | (-16) 22 (81) | (91) 192 (321) | (37) 130 (281) |
| | BIGI | (22) 61 (116) | (-9) 29 (101) | (95) 193 (323) | (54) 153 (321) |
| | OWY | (27) 79 (150) | (53) 309 (1576) | (81) 312 (395) | (227) 997 (5000) |
| | SNYI | (10) 32 (50) | (-3) 21 (44) | (44) 87 (158) | (17) 61 (131) |

| | | | | | |
|---|---|---|---|---|---|
| | DEDI | (1) 51 (114) | (-6) 3 (33) | (69) 204 (401) | (6) 50 (232) |
| | PABI | (24) 90 (154) | (-6) 23 (89) | (152) 281 (447) | (30) 109 (221) |
| | HRSI | (15) 61 (110) | (2) 31 (78) | (105) 201 (318) | (46) 116 (218) |
| | PRPI | (23) 69 (112) | (-17) 15 (57) | (140) 204 (311) | (17) 83 (164) |
| | WEII | (14) 39 (57) | (-1) 21 (41) | (59) 104 (176) | (28) 70 (141) |
| | BRN | (14) 39 (59) | (-3) 23 (43) | (61) 107 (176) | (30) 71 (139) |
| | OXB | (14) 39 (59) | (-3) 23 (43) | (61) 107 (176) | (30) 71 (139) |
| Lower Snake | ANA | (12) 34 (60) | (0) 25 (46) | (57) 103 (171) | (35) 74 (143) |
| | DWR | (20) 64 (97) | (-10) 15 (44) | (121) 187 (260) | (18) 44 (80) |
| | SPD | (18) 61 (104) | (0) 37 (73) | (111) 169 (256) | (58) 92 (160) |
| | LWG | (8) 36 (63) | (-2) 22 (48) | (67) 106 (168) | (39) 74 (134) |
| | LGS | (8) 36 (63) | (-2) 22 (48) | (67) 106 (168) | (39) 74 (134) |
| | LMN | (9) 39 (67) | (-2) 24 (51) | (72) 113 (176) | (42) 79 (141) |
| | IHR | (9) 39 (67) | (-2) 24 (51) | (71) 113 (176) | (42) 79 (141) |
| | MCN | (9) 31 (57) | (-2) 11 (23) | (59) 95 (152) | (12) 29 (57) |
| Lower Columbia | JDA | (8) 32 (56) | (-1) 11 (24) | (60) 95 (150) | (14) 31 (58) |
| | TDA | (8) 31 (56) | (-1) 12 (25) | (59) 92 (146) | (14) 31 (58) |
| | BON | (8) 32 (56) | (-1) 13 (26) | (61) 91 (142) | (15) 32 (59) |
| Willamette | SVN | (2) 16 (27) | (2) 17 (28) | (22) 28 (40) | (23) 29 (41) |

**Table S4.** March-May (MAM) Volume Percent Change. U is unregulated, R is regulated. Table shows the (10th) 50th (90th) percentiles of the ensemble. For each region, locations are sorted from upstream (top) to downstream (bottom) based on position of tributary confluence with the next lowest order stream using a top-down stream order approach (e.g., a headwater tributary has a higher stream order than the mainstem).

**MAM**

| Region | Site ID | 2030 U | 2030 R | 2070 U | 2070 R |
|---|---|---|---|---|---|
| Upper Columbia | MCD | (18) 33 (57) | (0) 17 (42) | (59) 95 (151) | (17) 63 (110) |
| | RVC | (19) 30 (56) | (10) 23 (43) | (58) 92 (142) | (42) 70 (114) |
| | ARD | (16) 28 (50) | (2) 21 (46) | (49) 78 (119) | (34) 55 (95) |
| | MUC | (9) 26 (43) | (3) 22 (39) | (43) 65 (96) | (38) 52 (88) |
| Kootenai | LIB | (7) 29 (46) | (1) 23 (38) | (42) 67 (106) | (33) 49 (75) |
| | BFE | (5) 25 (38) | (1) 21 (33) | (35) 54 (80) | (28) 42 (65) |
| | DCD | (13) 35 (58) | (9) 41 (79) | (51) 89 (145) | (77) 140 (214) |
| | CAN | (6) 27 (40) | (4) 25 (42) | (36) 60 (87) | (39) 58 (91) |
| | BRI | (6) 27 (41) | (4) 26 (42) | (36) 60 (88) | (39) 58 (93) |
| Pend Oreille | HGH | (17) 38 (61) | (0) 10 (23) | (49) 79 (118) | (8) 25 (56) |
| | CFM | (14) 34 (54) | (8) 24 (38) | (42) 70 (100) | (33) 50 (78) |

| | | | | | |
|---|---|---|---|---|---|
| | KER | (13) 33 (51) | (9) 27 (45) | (42) 67 (97) | (42) 60 (99) |
| | TOM | (12) 31 (44) | (8) 29 (41) | (39) 56 (80) | (38) 55 (84) |
| | NOX | (12) 30 (44) | (8) 29 (41) | (38) 56 (79) | (38) 55 (84) |
| | CAB | (11) 29 (43) | (8) 28 (40) | (36) 54 (75) | (36) 53 (81) |
| | PSL | (5) 17 (28) | (9) 27 (42) | (10) 28 (49) | (28) 50 (76) |
| | ALF | (9) 25 (38) | (8) 28 (42) | (29) 47 (68) | (38) 56 (87) |
| | BOX | (9) 25 (37) | (8) 28 (42) | (28) 46 (67) | (39) 56 (87) |
| | BDY | (9) 25 (37) | (8) 28 (42) | (28) 46 (67) | (38) 57 (86) |
| | SEV | (8) 25 (37) | (8) 28 (42) | (27) 46 (67) | (37) 56 (86) |
| Spokane | PFL | (-8) 1 (11) | (-4) 5 (18) | (-23) -9 (17) | (-16) 0 (33) |
| | MON | (-7) 1 (10) | (-4) 6 (18) | (-21) -9 (17) | (-14) 2 (33) |
| | NIN | (-7) 1 (10) | (-4) 6 (18) | (-20) -7 (18) | (-13) 3 (33) |
| | LFL | (-7) 1 (10) | (-4) 6 (17) | (-19) -6 (19) | (-12) 3 (33) |
| Middle Columbia | GCL | (7) 23 (35) | (3) 21 (29) | (33) 50 (73) | (27) 41 (65) |
| | CHL | (9) 32 (61) | (12) 55 (93) | (49) 77 (147) | (98) 152 (241) |
| | CHJ | (7) 23 (35) | (3) 21 (29) | (33) 50 (74) | (27) 41 (65) |
| | WEL | (7) 24 (35) | (2) 22 (29) | (33) 50 (74) | (30) 42 (64) |
| | RRH | (7) 25 (35) | (2) 23 (29) | (35) 52 (75) | (32) 44 (65) |
| | RIS | (7) 24 (35) | (2) 23 (29) | (35) 52 (74) | (32) 45 (64) |
| | WAN | (7) 25 (35) | (2) 23 (29) | (35) 52 (75) | (33) 45 (65) |
| | PRD | (7) 25 (35) | (2) 23 (29) | (35) 52 (75) | (33) 46 (65) |
| Yakima | KEE | (-2) 8 (18) | (-14) 0 (16) | (-24) -5 (17) | (-20) 8 (26) |
| | KAC | (-2) 7 (17) | (-39) -11 (14) | (-28) -5 (19) | (-37) -2 (25) |
| | CLE | (18) 36 (60) | (-11) 4 (25) | (37) 61 (110) | (18) 43 (99) |
| | BUM | (10) 27 (49) | (13) 37 (70) | (7) 30 (59) | (26) 60 (85) |
| | RIM | (0) 13 (29) | (-18) 0 (31) | (-10) 16 (41) | (-9) 16 (52) |
| Upper Snake | JCKY | (17) 44 (78) | (15) 57 (119) | (71) 93 (164) | (107) 161 (312) |
| | PALI | (14) 32 (61) | (9) 28 (58) | (45) 75 (134) | (44) 69 (128) |
| | HEII | (13) 30 (59) | (9) 27 (56) | (42) 72 (129) | (42) 66 (123) |
| | LORI | (13) 30 (59) | (10) 32 (69) | (42) 72 (129) | (50) 82 (148) |
| | REXI | (11) 27 (56) | (14) 35 (69) | (37) 60 (109) | (43) 74 (136) |
| | SHYI | (14) 31 (60) | (13) 36 (75) | (48) 72 (129) | (59) 90 (164) |
| | BFTI | (14) 31 (62) | (16) 42 (85) | (49) 73 (132) | (66) 102 (188) |
| | AMFI | (12) 30 (61) | (19) 33 (63) | (45) 71 (122) | (57) 82 (159) |
| | MILI | (13) 30 (59) | (30) 66 (117) | (43) 73 (118) | (97) 162 (264) |
| | KIMI | (13) 29 (58) | (29) 63 (110) | (42) 72 (116) | (91) 154 (248) |
| | SKHI | (14) 26 (49) | (15) 36 (65) | (35) 64 (101) | (51) 89 (144) |
| | SWAI | (13) 27 (49) | (16) 37 (67) | (33) 62 (96) | (50) 89 (140) |
| | ANDI | (10) 30 (70) | (21) 49 (81) | (28) 54 (147) | (60) 98 (169) |
| | ARKI | (9) 26 (46) | (19) 42 (63) | (22) 45 (93) | (48) 74 (125) |

| | | | | | |
|---|---|---|---|---|---|
| | LUCI | (9) 25 (47) | (19) 42 (66) | (18) 44 (88) | (48) 76 (136) |
| | BIGI | (10) 24 (46) | (23) 57 (96) | (18) 43 (85) | (66) 107 (204) |
| | OWY | (-8) 21 (65) | (-3) 55 (137) | (0) 40 (153) | (27) 87 (259) |
| | SNYI | (12) 28 (47) | (20) 45 (74) | (30) 63 (92) | (55) 99 (172) |
| | DEDI | (26) 45 (133) | (-1) 59 (141) | (43) 73 (356) | (92) 170 (317) |
| | PABI | (7) 21 (36) | (11) 30 (52) | (3) 28 (64) | (25) 54 (91) |
| | HRSI | (12) 25 (56) | (7) 20 (50) | (13) 34 (110) | (11) 35 (118) |
| | PRPI | (9) 24 (52) | (1) 17 (54) | (14) 32 (97) | (6) 32 (124) |
| | WEII | (10) 25 (43) | (12) 34 (58) | (25) 54 (84) | (36) 74 (134) |
| | BRN | (10) 25 (42) | (12) 32 (59) | (24) 52 (81) | (35) 72 (135) |
| | OXB | (10) 24 (42) | (12) 32 (59) | (24) 51 (81) | (35) 72 (135) |
| Lower Snake | ANA | (15) 25 (41) | (18) 30 (49) | (28) 50 (82) | (38) 63 (103) |
| | DWR | (4) 14 (26) | (-2) 7 (19) | (-1) 11 (42) | (5) 16 (34) |
| | SPD | (5) 17 (30) | (3) 17 (26) | (5) 18 (47) | (9) 23 (43) |
| | LWG | (12) 22 (36) | (14) 25 (40) | (24) 44 (67) | (31) 53 (81) |
| | LGS | (13) 22 (36) | (15) 25 (40) | (24) 45 (68) | (32) 53 (82) |
| | LMN | (13) 23 (36) | (15) 26 (41) | (24) 45 (68) | (32) 54 (83) |
| | IHR | (13) 23 (37) | (15) 26 (41) | (24) 45 (69) | (32) 54 (83) |
| | MCN | (7) 24 (34) | (4) 25 (33) | (33) 48 (69) | (37) 47 (68) |
| Lower Columbia | JDA | (7) 25 (33) | (4) 25 (33) | (33) 48 (68) | (38) 47 (68) |
| | TDA | (7) 24 (33) | (4) 25 (32) | (33) 46 (67) | (37) 45 (66) |
| | BON | (7) 23 (32) | (4) 24 (31) | (32) 44 (64) | (34) 43 (63) |
| Willamette | SVN | (-15) -5 (0) | (-14) -4 (0) | (-22) -11 (1) | (-21) -10 (2) |

**Table S5.** June-August (JJA) Volume Percent Change. U is unregulated, R is regulated. Table shows the (10th) 50th (90th) percentiles of the ensemble. For each region, locations are sorted from upstream (top) to downstream (bottom) based on position of tributary confluence with the next lowest order stream using a top-down stream order approach (e.g., a headwater tributary has a higher stream order than the mainstem).

**JJA**

| Region | Site ID | 2030 U | 2030 R | 2070 U | 2070 R |
|---|---|---|---|---|---|
| Upper Columbia | MCD | (-9) -5 (-1) | (-2) 14 (25) | (-33) -20 (-6) | (3) 21 (39) |
| | RVC | (-10) -6 (-2) | (-8) 1 (8) | (-36) -23 (-8) | (-15) -4 (6) |
| | ARD | (-12) -8 (-4) | (-2) 4 (13) | (-39) -26 (-12) | (0) 12 (21) |
| | MUC | (-17) -12 (-8) | (-9) -5 (1) | (-45) -31 (-17) | (-17) -10 (-2) |
| Kootenai | LIB | (-22) -14 (-10) | (-14) -5 (2) | (-51) -37 (-20) | (-20) -9 (-1) |
| | BFE | (-23) -17 (-11) | (-19) -11 (-2) | (-52) -39 (-22) | (-31) -19 (-13) |
| | DCD | (-10) -6 (-1) | (-4) 3 (21) | (-38) -24 (-9) | (-30) -11 (16) |
| | CAN | (-22) -16 (-10) | (-18) -11 (-5) | (-53) -39 (-21) | (-39) -28 (-15) |

| | | | | | |
|---|---|---|---|---|---|
| | BRI | (-23) -16 (-11) | (-19) -12 (-7) | (-54) -40 (-22) | (-42) -30 (-17) |
| Pend Oreille | HGH | (-34) -22 (-13) | (-15) 1 (24) | (-65) -54 (-31) | (-12) 0 (17) |
| | CFM | (-31) -23 (-14) | (-26) -16 (-11) | (-63) -53 (-31) | (-51) -39 (-24) |
| | KER | (-31) -22 (-13) | (-25) -16 (-8) | (-62) -51 (-30) | (-48) -38 (-23) |
| | TOM | (-29) -20 (-13) | (-27) -17 (-10) | (-60) -45 (-28) | (-54) -41 (-26) |
| | NOX | (-30) -21 (-13) | (-29) -18 (-11) | (-61) -47 (-29) | (-56) -43 (-27) |
| | CAB | (-30) -21 (-13) | (-28) -18 (-11) | (-60) -46 (-29) | (-55) -42 (-27) |
| | PSL | (-40) -30 (-17) | (-40) -29 (-15) | (-67) -54 (-38) | (-69) -56 (-34) |
| | ALF | (-30) -21 (-13) | (-29) -19 (-11) | (-58) -45 (-28) | (-56) -43 (-27) |
| | BOX | (-29) -21 (-13) | (-28) -19 (-10) | (-58) -44 (-28) | (-55) -42 (-26) |
| | BDY | (-29) -21 (-13) | (-28) -19 (-10) | (-58) -44 (-28) | (-55) -42 (-26) |
| | SEV | (-29) -21 (-13) | (-28) -19 (-10) | (-58) -45 (-28) | (-55) -42 (-26) |
| Spokane | PFL | (-49) -38 (-21) | (-52) -41 (-23) | (-72) -61 (-49) | (-75) -65 (-54) |
| | MON | (-44) -34 (-19) | (-49) -38 (-22) | (-67) -55 (-44) | (-73) -62 (-50) |
| | NIN | (-42) -32 (-18) | (-46) -36 (-21) | (-63) -52 (-40) | (-70) -58 (-46) |
| | LFL | (-40) -30 (-17) | (-44) -33 (-20) | (-61) -50 (-38) | (-67) -55 (-43) |
| Middle Columbia | GCL | (-20) -14 (-10) | (-15) -9 (-3) | (-48) -36 (-22) | (-27) -18 (-11) |
| | CHL | (-31) -14 (-4) | (-49) -19 (-1) | (-63) -40 (-15) | (-88) -64 (-19) |
| | CHJ | (-20) -14 (-9) | (-14) -9 (-3) | (-48) -36 (-22) | (-27) -18 (-11) |
| | WEL | (-21) -14 (-10) | (-15) -10 (-4) | (-49) -37 (-22) | (-29) -19 (-14) |
| | RRH | (-21) -14 (-10) | (-16) -10 (-4) | (-49) -37 (-22) | (-31) -20 (-15) |
| | RIS | (-21) -15 (-10) | (-17) -10 (-5) | (-50) -37 (-22) | (-32) -21 (-16) |
| | WAN | (-21) -14 (-10) | (-17) -10 (-5) | (-50) -37 (-22) | (-32) -21 (-15) |
| | PRD | (-21) -14 (-10) | (-17) -10 (-5) | (-50) -37 (-22) | (-32) -21 (-16) |
| Yakima | KEE | (-63) -42 (-24) | (0) 6 (16) | (-81) -68 (-43) | (-2) 12 (28) |
| | KAC | (-62) -41 (-25) | (-1) 10 (35) | (-80) -69 (-46) | (5) 37 (80) |
| | CLE | (-41) -24 (-11) | (3) 6 (12) | (-80) -59 (-29) | (-4) 7 (13) |
| | BUM | (-53) -34 (-20) | (-41) -25 (-13) | (-81) -64 (-39) | (-67) -51 (-27) |
| | RIM | (-37) -25 (-14) | (-4) 1 (6) | (-64) -47 (-27) | (-8) 1 (8) |
| Upper Snake | JCKY | (-27) -14 (-1) | (-12) -5 (4) | (-56) -43 (-17) | (-31) -18 (-3) |
| | PALI | (-25) -13 (0) | (-11) -3 (5) | (-49) -37 (-14) | (-26) -16 (-2) |
| | HEII | (-24) -12 (0) | (-11) -3 (5) | (-47) -36 (-14) | (-26) -16 (-2) |
| | LORI | (-24) -12 (0) | (-16) -4 (10) | (-47) -36 (-14) | (-38) -24 (-3) |
| | REXI | (-17) -9 (0) | (-18) -9 (1) | (-40) -29 (-9) | (-40) -29 (-9) |
| | SHYI | (-22) -11 (0) | (-19) -6 (8) | (-45) -34 (-12) | (-47) -33 (-7) |
| | BFTI | (-22) -11 (0) | (-27) -7 (11) | (-46) -35 (-12) | (-63) -45 (-8) |
| | AMFI | (-21) -10 (1) | (-2) 4 (11) | (-43) -32 (-10) | (-13) -7 (9) |
| | MILI | (-20) -10 (1) | (-24) 8 (52) | (-44) -32 (-10) | (-79) -47 (31) |
| | KIMI | (-19) -10 (1) | (-20) 8 (46) | (-43) -31 (-10) | (-69) -40 (29) |
| | SKHI | (-15) -7 (4) | (-5) 9 (25) | (-36) -23 (-4) | (-16) -1 (29) |

| | | | | | |
|---|---|---|---|---|---|
| | SWAI | (-14) -5 (6) | (-7) 8 (23) | (-33) -18 (0) | (-20) -1 (32) |
| | ANDI | (-27) -12 (3) | (-17) -7 (6) | (-53) -35 (-8) | (-30) -19 (1) |
| | ARKI | (-27) -12 (0) | (-15) -7 (3) | (-52) -35 (-8) | (-33) -19 (-1) |
| | LUCI | (-27) -12 (0) | (-13) -5 (3) | (-52) -36 (-10) | (-29) -16 (0) |
| | BIGI | (-27) -11 (0) | (-20) -9 (12) | (-51) -34 (-8) | (-42) -24 (10) |
| | OWY | (-24) 6 (58) | (-11) 0 (23) | (-30) 4 (110) | (-18) -1 (37) |
| | SNYI | (-15) -5 (6) | (-10) 5 (24) | (-33) -16 (2) | (-24) -2 (29) |
| | DEDI | (-39) -20 (-6) | (-10) -1 (10) | (-65) -54 (-29) | (-21) -11 (2) |
| | PABI | (-40) -23 (-10) | (-18) -6 (1) | (-69) -53 (-30) | (-34) -23 (-3) |
| | HRSI | (-32) -18 (-7) | (-22) -12 (-3) | (-61) -47 (-26) | (-41) -29 (-13) |
| | PRPI | (-34) -18 (-7) | (-34) -16 (-4) | (-61) -47 (-25) | (-58) -42 (-16) |
| | WEII | (-16) -6 (3) | (-16) -1 (12) | (-36) -19 (-1) | (-32) -12 (14) |
| | BRN | (-17) -6 (3) | (-15) -1 (11) | (-36) -19 (-1) | (-30) -12 (14) |
| | OXB | (-17) -6 (3) | (-15) -1 (11) | (-36) -19 (-1) | (-30) -12 (14) |
| Lower Snake | ANA | (-22) -10 (-2) | (-24) -9 (-1) | (-45) -30 (-10) | (-48) -30 (-7) |
| | DWR | (-41) -29 (-18) | (-6) -1 (4) | (-67) -56 (-42) | (-15) -7 (-1) |
| | SPD | (-41) -25 (-18) | (-27) -16 (-10) | (-69) -55 (-40) | (-48) -36 (-26) |
| | LWG | (-26) -13 (-6) | (-24) -9 (-4) | (-48) -34 (-15) | (-45) -29 (-11) |
| | LGS | (-26) -13 (-6) | (-24) -9 (-3) | (-48) -34 (-15) | (-45) -29 (-11) |
| | LMN | (-28) -13 (-7) | (-26) -11 (-4) | (-50) -36 (-16) | (-48) -32 (-13) |
| | IHR | (-28) -13 (-7) | (-27) -11 (-4) | (-50) -36 (-16) | (-48) -32 (-13) |
| | MCN | (-21) -14 (-11) | (-17) -10 (-6) | (-49) -34 (-21) | (-36) -24 (-15) |
| Lower Columbia | JDA | (-21) -14 (-11) | (-17) -10 (-6) | (-49) -34 (-21) | (-36) -23 (-15) |
| | TDA | (-21) -14 (-11) | (-17) -10 (-6) | (-49) -34 (-21) | (-36) -23 (-15) |
| | BON | (-21) -14 (-11) | (-17) -10 (-6) | (-49) -34 (-21) | (-35) -23 (-15) |
| Willamette | SVN | (-38) -25 (-16) | (-35) -22 (-13) | (-58) -40 (-25) | (-54) -35 (-22) |